

# Methylator-induced, Mismatch Repair-dependent G<sub>2</sub> Arrest Is Activated through Chk1 and Chk2

Aaron W. Adamson,<sup>\*†‡</sup> Dillon I. Beardsley,<sup>\*†§</sup> Wan-Ju Kim,<sup>†§</sup> Yajuan Gao,<sup>||</sup>  
R. Baskaran,<sup>||</sup> and Kevin D. Brown<sup>§</sup>

<sup>\*</sup>Department of Biochemistry and Molecular Biology and the Stanley S. Scott Cancer Center, Louisiana State University Health Sciences Center, New Orleans, LA 70112; <sup>§</sup>Department of Biochemistry and Molecular Biology and the Shands Cancer Center, University of Florida College of Medicine, Gainesville, FL 32610; and <sup>||</sup>Department of Molecular Genetics and Biochemistry, University of Pittsburgh Medical Center, Pittsburgh, PA 15261

Submitted February 3, 2004; Revised December 13, 2004; Accepted December 21, 2004  
Monitoring Editor: Tony Hunter

S<sub>N</sub>1 DNA methylating agents such as the nitrosourea *N*-methyl-*N'*-nitro-*N*-nitrosoguanidine (MNNG) elicit a G<sub>2</sub>/M checkpoint response via a mismatch repair (MMR) system-dependent mechanism; however, the exact nature of the mechanism governing MNNG-induced G<sub>2</sub>/M arrest and how MMR mechanistically participates in this process are unknown. Here, we show that MNNG exposure results in activation of the cell cycle checkpoint kinases ATM, Chk1, and Chk2, each of which has been implicated in the triggering of the G<sub>2</sub>/M checkpoint response. We document that MNNG induces a robust, dose-dependent G<sub>2</sub> arrest in MMR and ATM-proficient cells, whereas this response is abrogated in MMR-deficient cells and attenuated in ATM-deficient cells treated with moderate doses of MNNG. Pharmacological and RNA interference approaches indicated that Chk1 and Chk2 are both required components for normal MNNG-induced G<sub>2</sub> arrest. MNNG-induced nuclear exclusion of the cell cycle regulatory phosphatase Cdc25C occurred in an MMR-dependent manner and was compromised in cells lacking ATM. Finally, both Chk1 and Chk2 interact with the MMR protein MSH2, and this interaction is enhanced after MNNG exposure, supporting the notion that the MMR system functions as a molecular scaffold at the sites of DNA damage that facilitates activation of these kinases.

## INTRODUCTION

Cells are continually exposed to numerous forces and toxins capable of damaging DNA. To ensure maintenance of genome stability, cells have evolved a complex set of mechanisms to appropriately respond to genotoxic damage. Such responses include genome surveillance and DNA repair, activation of cell cycle checkpoints, and apoptosis. Tumor initiation and progression are directly linked to genomic instability and often correlate with loss of gene(s) involved in genome damage response (Hartwell and Kastan, 1994; Loeb *et al.*, 2003). Paradoxically, many cancer treatment regimens induce DNA damage and exert their therapeutic effects through activation of growth arrest or apoptotic responses. Thus, elucidating the mechanisms and molecules that govern DNA damage response is key to understanding the molecular basis of both tumor formation and the therapeutic effects of many anticancer drugs.

The nitrosourea *N*-methyl-*N'*-nitro-*N*-nitrosoguanidine (MNNG) is a well characterized monofunctional DNA alkylating agent. The cytotoxic and mutagenic potential of

MNNG is chiefly attributable to its ability to alkylate (methylate) the O<sup>6</sup>-position of guanine, resulting in formation of O<sup>6</sup>-methylguanine (O<sup>6</sup>MeG) adducts (Goldmacher *et al.*, 1986; Karran and Bignami, 1992). O<sup>6</sup>MeG forces O<sup>6</sup>MeG-T mispairing after DNA replication due to blocking of a hydrogen bonding position involved in complementary base pairing. This mutagenic lesion is primarily repaired via direct demethylation by the DNA repair protein methylguanine-DNA methyltransferase (MGMT) (Lindahl *et al.*, 1982). Moreover, loss of MGMT activity renders cells extremely sensitive to MNNG and like alkylators (Kalamegham *et al.*, 1988), underscoring the role that O<sup>6</sup>MeG lesions play in triggering response to this drug. O<sup>6</sup>MeG lesions are also recognized and repaired by the mismatch repair (MMR) system (Griffin *et al.*, 1994; Duckett *et al.*, 1996).

In response to MNNG and other methylators, cells undergo a robust G<sub>2</sub>/M arrest (Plant and Roberts, 1971; Goldmacher *et al.*, 1986), in contrast to ionizing radiation (IR) and UV light, which trigger both G<sub>1</sub>/S and G<sub>2</sub>/M checkpoints (Kastan *et al.*, 1991; Kaufmann and Wilson, 1994). Furthermore, unlike response to IR, which results in establishment of growth arrest within hours after exposure, cells treated with MNNG undergo arrest in a delayed manner correlating with the observation that cells progress through one cell division before arresting after the second S phase after drug exposure (Plant and Roberts, 1971; Goldmacher *et al.*, 1986; Zhukovskaya *et al.*, 1994). Although little is known concerning the pathways that govern cell cycle checkpoint activation in response to alkylation-induced DNA damage, numerous groups have shown that activation of G<sub>2</sub>/M arrest in response to such genotoxins is dependent upon a functional

This article was published online ahead of print in *MBC in Press* (<http://www.molbiolcell.org/cgi/doi/10.1091/mbc.E04-02-0089>) on January 12, 2005.

<sup>†</sup> These authors contributed equally to this work.

<sup>‡</sup> Present address: Pennington Biomedical Research Center, 6400 Perkins Rd., Baton Rouge, LA 70808.

Address correspondence to: Kevin D. Brown ([kdbrown1@ufl.edu](mailto:kdbrown1@ufl.edu)).

MMR system (Goldmacher *et al.*, 1986; Kat *et al.*, 1993; Koi *et al.*, 1994). The inability of MMR-deficient cells to trigger either growth arrest or apoptotic response to methylators renders these cells significantly less sensitive to the cytotoxic effects of these genotoxins, and this phenotypic effect has been termed alkylation tolerance (Branch *et al.*, 1993; Kat *et al.*, 1993). Although the molecular basis for the alkylation tolerance phenotype has yet to be fully elucidated, several recent reports indicate that the MMR system plays an active role in triggering response to DNA damage (Brown *et al.*, 2003; Cejka *et al.*, 2003; Hirose *et al.*, 2003; Wang and Qin, 2003). However, the signaling mechanisms that govern MNNG-induced growth arrest and the nature of MMR-dependent step(s) that facilitate this arrest remain, in general, poorly defined.

As a result of much focused effort, pathways that govern the G<sub>2</sub>/M checkpoint in response to IR have been partially elucidated. Among the key players in IR-induced checkpoint response are the high-molecular-weight PIK-like kinases ATM and ATR (Abraham, 2001). In response to DNA damage, ATR phosphorylates and consequently activates the kinase Chk1 (Liu *et al.*, 2000). In turn, Chk1 phosphorylates the phosphatase Cdc25C on residue Ser216 (Sanchez *et al.*, 1997), which induces binding of Cdc25C with the molecular chaperone 14-3-3 (Peng *et al.*, 1997), resulting in the cytoplasmic sequestration of Cdc25C (Dalal *et al.*, 1999; Graves *et al.*, 2000). Whereas Cdc25C dephosphorylates residues on the kinase Cdc2 leading to the catalytic activation of the Cdc2/cyclinB complex within the nucleus (Strausfeld *et al.*, 1991; Lee *et al.*, 1992), redistribution of the Cdc25C phosphatase to the cytoplasm results in an inhibition of mitotic entry and forms the basis for IR-induced G<sub>2</sub>/M arrest. Unsurprisingly, cells that contain diminished ATR (Cliby *et al.*, 1998; Wright *et al.*, 1998) or Chk1 (Liu *et al.*, 2000) activity show a clear defect in the triggering of the G<sub>2</sub>/M checkpoint in response to IR.

Several lines of investigation suggest that the ATR-related kinase ATM also may be involved in a parallel G<sub>2</sub>/M checkpoint pathway. In response to IR-induced DNA damage, the kinase Chk2 is activated through ATM-dependent phosphorylation (Matsuoka *et al.*, 1998; Ahn *et al.*, 2000; Matsuoka *et al.*, 2000). Chk2, like the functionally related but structurally dissimilar Chk1 kinase, also phosphorylates Cdc25C on Ser216 (Matsuoka *et al.*, 1998; Brown *et al.*, 1999), leading to the notion that ATM and Chk2 can promote IR-induced G<sub>2</sub>/M arrest by inhibiting Cdc2 kinase activity through cytoplasmic Cdc25C sequestration. However, cells deficient in ATM show no gross defects in the triggering of G<sub>2</sub>/M arrest in response to IR; rather, these cells are unable to halt mitotic advance immediately after irradiation (Zampetti-Bosseler and Scott, 1981; Paules *et al.*, 1995; Xu *et al.*, 2002). Likewise, cells deficient in Chk2 are able to trigger the G<sub>2</sub>/M checkpoint in response to IR (Jallepalli *et al.*, 2003). Thus, current data support the existence of an ATM/Chk2-dependent G<sub>2</sub>/M checkpoint mechanism; however, conditions that require this pathway to elicit G<sub>2</sub>/M arrest have yet to be described.

As mentioned above, the mechanisms that control MNNG-induced G<sub>2</sub>/M arrest, as well as the essential role that MMR plays in this process, are unknown. However, a number of potentially important recent developments have begun to shed light on this topic. For example, our laboratory showed that MNNG exposure results in the catalytic activation of ATM through a MMR-independent mechanism (Adamson *et al.*, 2002). We also recently reported that MMR-deficient cells display defective Chk2 activation in response to IR exposure (Brown *et al.*, 2003). Moreover, using both in

vitro and in vivo approaches, we found that ATM and Chk2 associate with MMR proteins, prompting us to propose that the assembly of an MMR complex at the site of DNA damage results in establishment of a molecular scaffold that facilitates phosphorylation of Chk2 by ATM. Similarly, Wang and Qin (2003) recently showed an MMR dependence to Chk1 activation. These advances led us to hypothesize that defective activation of Chk1/Chk2 may underlie faulty G<sub>2</sub>/M checkpoint activation in response to methylating agents. This article outlines our work aimed at testing this hypothesis, and the results stemming from this study advance our understanding of the mechanisms involved in alkylation tolerance, genetic instability, and cancer predisposition arising from inactivation of the MMR system.

## MATERIALS AND METHODS

### Cell Culture and Drug Treatment

Normal human diploid foreskin fibroblasts (NHFs) were established from circumcision specimens and cultured in DMEM supplemented with 10% fetal bovine serum. Experimentation was generally conducted on NHFs at passage 6. The SV40-immortalized A-T fibroblast line AT221JE-T stably expressing full-length recombinant human ATM (designated YZ-5) or stably transfected with empty vector (designated EBS-7) was cultured as indicated previously (Ziv *et al.*, 1997). The MLH1-deficient human colorectal adenocarcinoma line HCT116 and its derivatives (HCT116+ch2, HCT116+ch3), and the MSH2-deficient endometrial adenocarcinoma tumor line HEC59 and its derivative (HEC59+ch2), were cultured with or without 400  $\mu$ g/ml G418 as outlined previously (Koi *et al.*, 1994; Umar *et al.*, 1997). All cell lines were grown at 37°C in a humidified 5% CO<sub>2</sub> incubator. ATM, MLH1, or MSH2 expression was confirmed by immunoblotting.

MNNG treatments were performed by removing media from cultures of logarithmically growing cells and adding serum-free media. MNNG was then added to the indicated final concentration, and cells were returned to the incubator. After a 1-h drug exposure, the plates were rinsed extensively with phosphate-buffered saline (PBS), and cells were refed on complete growth media and returned to the incubator. MNNG (Aldrich Chemical, Milwaukee, WI) was dissolved in 0.1 M Na-acetate, pH 5.0, at a stock concentration of 10 mM and stored at -20°C. 7-Hydroxystaurosporine (UCN-01) was obtained from the Developmental Therapeutics Program (National Cancer Institute, National Institutes of Health, Bethesda, MD). A 10 mM stock solution of this drug was stored at -80°C. UCN-01 was added to cell cultures (500 nM final concentration) 45 min before MNNG treatment. Cells were maintained on UCN-01 both during and after MNNG exposure until cells were harvested and analyzed. Caffeine (Sigma-Aldrich, St. Louis, MO) was diluted in PBS at a stock concentration of 100 mM and stored at room temperature (RT). Caffeine (5 mM final concentration) was added 1 h before MNNG treatment and was maintained in the medium during and after MNNG exposure.

### Flow Cytometry

For analysis of total DNA content, cells were harvested by trypsinization, washed with PBS, fixed in ice-cold 70% ethanol, and stored at -20°C for a minimum of 24 h. Before analysis, cells were washed twice in PBS followed by a 30-min RT incubation in PBS containing 25  $\mu$ g/ml propidium iodide (PI) and 100  $\mu$ g/ml RNase A. Cells were analyzed using a BD Biosciences FAC-SCalibur flow cytometer, and 10,000 events were plotted using CellQuest software.

For quantitative assessment of G<sub>2</sub> arrest, a modification of the assay outlined by Xu *et al.* (2002) was used. Cells were treated with the indicated dose of MNNG and 48 h after exposure, demecolcine (Sigma-Aldrich) was added to the media (0.4  $\mu$ g/ml final concentration) and cells were returned to the incubator. After an additional 24-h incubation, both adherent and floating cells were harvested and fixed in ice-cold 70% ethanol. After fixation, cells were washed twice in PBS, suspended in 1 ml of PBS containing 0.25% Triton X-100, and incubated on ice for 5 min. Cells were collected by centrifugation, and the cell pellet was resuspended in 100  $\mu$ l of PBS containing 1% bovine serum albumin and 1  $\mu$ g of anti-histone H3 that recognizes this antigen when in the mitosis-specific phosphorylated (Ser10) state (06-570; Upstate Biotechnology, Lake Placid, NY). Cells were incubated with this antibody for 3 h at RT, rinsed, and subsequently incubated with fluorescein isothiocyanate (FITC)-conjugated goat anti-rabbit secondary antibody. After a 30-min RT incubation, the cells were washed in PBS, resuspended in PBS containing 25  $\mu$ g/ml PI and 100  $\mu$ g/ml RNase A, and incubated for 30 min at RT. Both FITC and PI fluorescence were simultaneously measured by flow cytometry.

### Immunoblot Analysis

SDS-PAGE and immunoblotting procedures were conducted as outlined previously (Adamson *et al.*, 2002). Membranes were probed with antibodies

directed against total ATM (AM-9; Allen *et al.*, 2001), phospho-Ser1981 ATM (600-401-400; Rockland, Gilbertsville, PA), total Chk1 (sc-8408; Santa Cruz Biotechnology, Santa Cruz, CA), phospho-Ser317 Chk1 (2344; Cell Signaling Technology, Beverly, MA), total Chk2 (sc-17748; Santa Cruz Biotechnology), phospho-Thr68 Chk2 (sc-16297-R; Santa Cruz Biotechnology), total Cdc2 (sc-54; Santa Cruz Biotechnology), phospho-Tyr15 Cdc2 (9111; Cell Signaling Technology), Cdc25C (sc-327; Santa Cruz Biotechnology), Cdc25A (sc-97; Santa Cruz Biotechnology), SMC1 (A300-055A; Bethyl Laboratories, Montgomery, TX), or tubulin (DM1A; a gift of Dr. D. W. Cleveland, Ludwig Institute, University of California San Diego) as indicated.

### Cell Fractionation

Cells were separated into nuclear and cytoplasmic fractions by using NE-PER nuclear and cytoplasmic extraction reagents as outlined by the manufacturer (Pierce Chemical, Rockford, IL). After lysing cells with supplied buffers, nuclei were harvested by centrifugation in a microcentrifuge (5 min, 16,000  $\times$  g, 4°C). Cytoplasmic (supernatant) and nuclear (pellet) fractions were separated and stored at -80°C before immunoblot analysis.

### RNA Interference (RNAi)

Pooled synthetic small interfering RNA (siRNA) duplexes (SMARTpool siRNA) specific for Chk1 (M-003255-01), Chk2 (M-003256-03), and luciferase (D-001120-01) were purchased from Dharmacon (Lafayette, CO). For siRNA transfection, HCT116+ch3 cells were seeded into six-well tissue culture plates at a density of  $5 \times 10^5$  cells/well 24 h before transfection. Just before transfection, medium was removed, and 1 ml of complete growth medium was added to each well. Subsequently, 200  $\mu$ l of reaction mix containing 5  $\mu$ l of 20  $\mu$ M siRNA and 2  $\mu$ l of Oligofectamine (Invitrogen, Carlsbad, CA) diluted in Opti-MEM was added to each well. After an overnight (O/N) incubation at 37°C, the cells were split at a 1:4 ratio and then cultured O/N. The next day, the cells were again transfected as outlined above. After this second transfection, the cells were washed, refed on complete growth medium, and treated with 5  $\mu$ M MNNG for 1 h. MNNG-treated cells were cultured for 48 h and subsequently harvested and fixed for flow cytometry or lysates formed for immunoblot analysis.

Alternatively, HCT116+ch3 cells were transfected with plasmids purchased from Upstate Biotechnology encoding short hairpin RNA (shRNA) specific for Chk1 (pKD-CHK1-v1), Chk2 (pKD-CHK2-v3), or the nonspecific control plasmid pKD-NegCon-v1. For these experiments,  $5 \times 10^5$  HCT116+ch3 cells/well were seeded into six-well plates and allowed to attach O/N. The next day, the media were removed, and 2 ml of DMEM + 10% fetal calf serum without antibiotics was added. To this, 500  $\mu$ l of serum-free Opti-MEM containing 12.5  $\mu$ l of LipofectAMINE 2000 (Invitrogen) and 5  $\mu$ g of plasmid DNA were added, and cells were returned to the incubator. Cells were cultured for 72 h and subsequently split at a 1:4 ratio. The next day, cells were treated with 5  $\mu$ M MNNG for 1 h and returned to the incubator. Cells were harvested for immunoblotting and flow cytometry analysis 48 h after drug treatment.

### Immunoprecipitation

Approximately  $1 \times 10^7$  HEC59 or HEC59+ch2 cells were either untreated or treated with 25  $\mu$ M MNNG for 1 h. After a 48-h incubation, cells were harvested, washed with ice-cold PBS, and lysed in 1 $\times$  lysis buffer (20 mM Tris-HCl, pH 7.5, 150 mM NaCl, 5 mM EDTA, 0.5% NP-40, 1 mM NaF, 1 mM dithiothreitol, 1 mM Na-vanadate, and 1 mM leupeptin and aprotinin). After preclearing, the lysates were adjusted for equal protein content, and 5  $\mu$ l of polyclonal rabbit MSH2 antisera (ab9146; Novus Biologicals, Littleton, CO) was added. After a 2-h incubation on ice, 10  $\mu$ l of a 50/50 slurry of protein A/G beads (Pfizer, New York, NY) in PBS was added, and the incubation was continued for 1 h with end-over-end rocking. Immunocomplexes were washed three times with 1 $\times$  lysis buffer containing 500 mM NaCl and twice with 1 $\times$  lysis buffer containing 100 mM NaCl. Immunocomplexes were finally resuspended in 1 $\times$  SDS-PAGE loading buffer and subjected to immunoblot analysis.

## RESULTS

### Activation of Chk1 and Chk2 Correlates with MNNG-induced G<sub>2</sub> Arrest

We hypothesize that faulty activation of Chk1/Chk2 is responsible for the cell cycle arrest defect shown by MMR-deficient cells in response to monofunctional alkylators. Our first test of this notion was to determine whether Chk1 and Chk2 were activated in response to MNNG and whether this correlates with G<sub>2</sub>/M arrest. We treated NHF with MNNG and saw no notable accumulation of cells with a 4N DNA content until 48 h after MNNG at which point a robust G<sub>2</sub>/M arrest was evident (Figure 1A). These results are

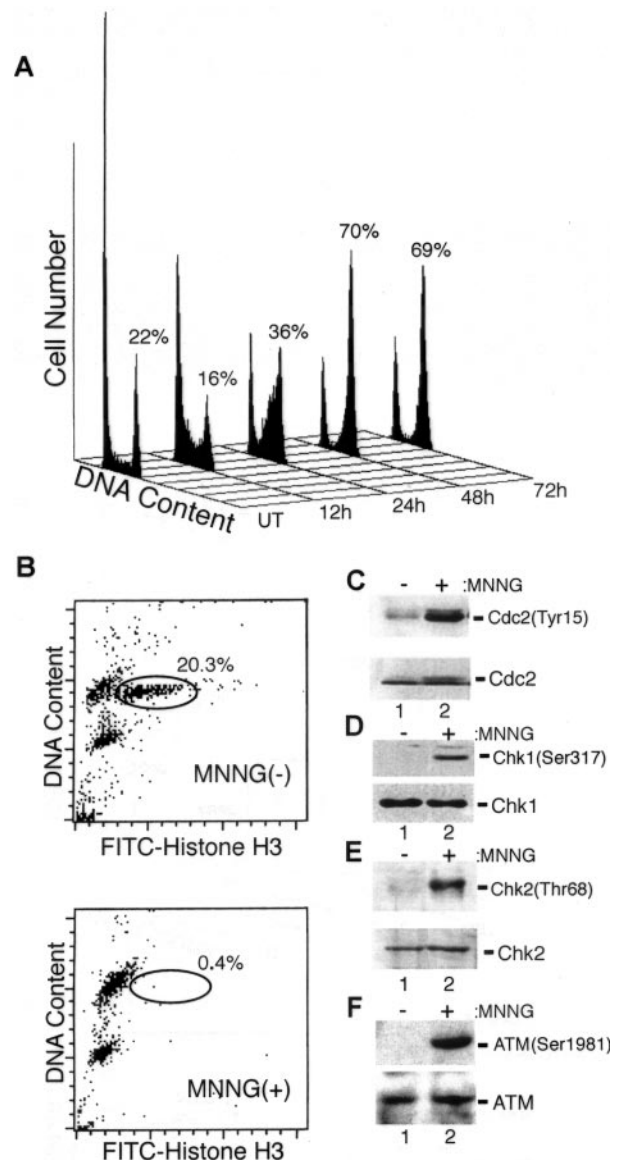


**Figure 1.** MNNG exposure results in G<sub>2</sub> arrest; activation of ATM, Chk1, and Chk2; and inactivation of Cdc2. (A) NHFs were either mock treated (UT) or treated with 25  $\mu$ M MNNG, harvested at the indicated time point, fixed, stained with propidium iodide, and analyzed by flow cytometry. The percentage of cells with a 4N DNA content is indicated. (B) Logarithmically growing NHFs were either mock treated (top) or treated with MNNG (bottom). Forty-eight hours after MNNG exposure, demecolcine was added to the media and after an additional 24-h incubation the cells were harvested, stained, and analyzed for total DNA content (*y*-axis) and phospho-histone H3 (*x*-axis). The mitotic cell population is circled and percentage of the total cell population is indicated. (C) Extracts were formed from mock-treated (lane 1) and MNNG-treated (lane 2) NHFs 48 h after drug exposure and immunoblotted with phospho-Tyr15 specific anti-Cdc2 (top) and anti-total Cdc2 (bottom) to ensure equal protein abundance. (D) Extracts from untreated (lane 1) and MNNG-treated (lane 2) NHFs were subjected to immunoblotting with phospho-Ser317-specific anti-Chk1 (top) and anti-total Chk1 (bottom). (E) Extracts from untreated (lane 1) and MNNG-treated (lane 2) NHFs were subjected to immunoblotting with phospho-Thr68-specific anti-Chk2 (top) and anti-total Chk2 (bottom). (F) Extracts from untreated (lane 1) and MNNG-treated (lane 2) NHFs were subjected to immunoblotting with phospho-Ser1981-specific anti-ATM (top) and anti-total ATM (bottom).

consistent with the observation that cells treated with MNNG and related alkylators transit through one complete cell cycle before undergoing arrest (Plant and Roberts, 1971; Goldmacher *et al.*, 1986; Zhukovskaya *et al.*, 1994). To ensure that this result represented arrest in the G<sub>2</sub> phase of the cell cycle, we treated NHFs with MNNG and 48 h later added demecolcine to the culture media. After a 24-h incubation, harvested cells were double stained for DNA and the mitotic marker phospho-histone H3 and subsequently analyzed by flow cytometry. In untreated NHFs, we found that 20.3% of the cells stained positive for histone H3 phosphorylation after demecolcine treatment, whereas only 0.4% of the MNNG-treated cells progressed into mitosis during this time period (Figure 1B). This outcome indicates that a robust G<sub>2</sub> blockade is established in response to MNNG.

Next, lysates from MNNG-treated NHFs were immunoblotted with an antibody to phosphorylated (phospho-Tyr15) Cdc2 (Figure 1C). This posttranslational modification is inhibitory to the catalytic activity of this cyclin-dependent kinase, and we observed accumulation of Tyr15-phosphorylated Cdc2 48 h after MNNG exposure (time point corresponding to maximal cell cycle arrest). These extracts also were probed with an antibody specific for phosphorylated Chk1 (phospho-Ser317), and a clear increase in Chk1 phosphorylation was noted in response to MNNG (Figure 1D). Ser317 phosphorylation is required for activation of Chk1 (Zhao and Piwnicka-Worms, 2001). Similarly, phosphorylation of Chk2 (phospho-Thr68) also was observed in response to MNNG (Figure 1E). Phosphorylation of the Thr68 residue is required for Chk2 catalytic activation (Ahn *et al.*, 2000; Matsuoka *et al.*, 2000). Consistent with our previous findings that MNNG-induced DNA alkylation activates ATM, we observed that MNNG treatment resulted in the autophosphorylation of ATM at the Ser1981 residue (Figure 1F). This event is directly linked to the activation of ATM kinase activity (Bakkenist and Kastan, 2003). In sum, these findings indicate that MNNG induces G<sub>2</sub> arrest and that this event coincides with activation of ATM, Chk1, and Chk2 as well as the inactivation of Cdc2.

#### MNNG-induced G<sub>2</sub> Arrest Is Defective in MMR and ATM-deficient Cells

We recently identified the MMR system as a key component in some aspects of ATM-dependent response to DNA damage (Brown *et al.*, 2003). Because it is well established that G<sub>2</sub>/M arrest in response to MNNG is MMR dependent, and ATM has been implicated in G<sub>2</sub>/M checkpoint signaling, we sought to determine whether ATM is also a component in activation of this checkpoint. We exposed matched sets of ATM proficient/deficient and MMR proficient/deficient lines to various concentrations of MNNG and assayed G<sub>2</sub>/M arrest 48 h after MNNG exposure by flow cytometry. As expected, exposure of MLH1-deficient HCT116+ch2 cells to 200 nM to 10  $\mu$ M MNNG resulted in no observed accumulation of these cells in G<sub>2</sub>/M (Figure 2A). In contrast, matched MLH1-proficient HCT116+ch3 cells treated with moderate doses of MNNG (5 and 10  $\mu$ M) activated the G<sub>2</sub>/M checkpoint. Lower doses of MNNG (200 nM and 1  $\mu$ M) failed to activate a robust checkpoint in these cells. The differences in response between HCT116+ch2 and HCT116+ch3 cells are consistent with the MMR-dependent nature of checkpoint signaling in response to this alkylator. At a higher MNNG dose (25  $\mu$ M), we observed that HCT116+ch2 cells showed G<sub>2</sub>/M accumulation roughly equivalent to that of HCT116+ch3 cells. This supports the recent findings of Jaiswal *et al.* (2004) showing that 25  $\mu$ M MNNG induces G<sub>2</sub>/M arrest in the parental HCT116 line.

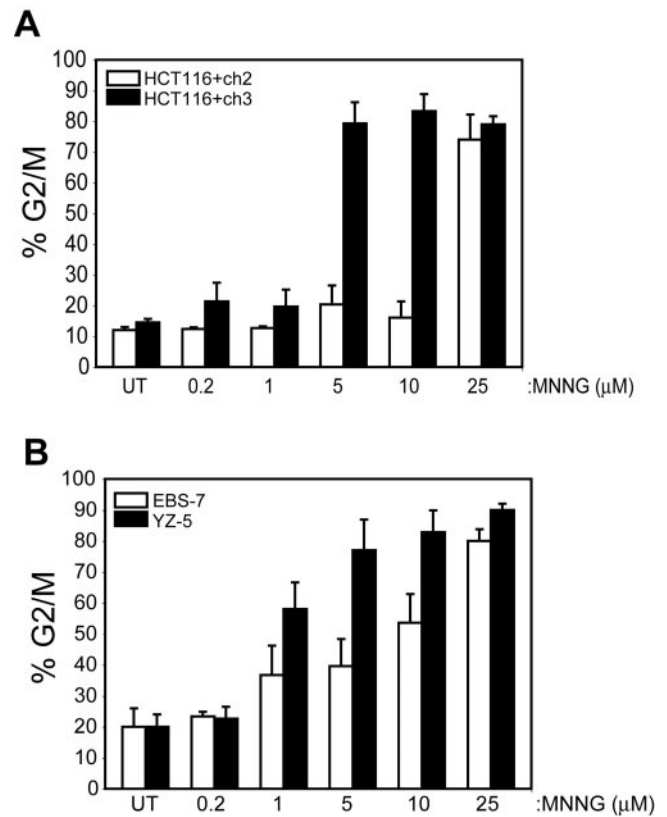


**Figure 2.** MNNG-induced G<sub>2</sub> arrest occurs through ATM- and MMR-dependent and -independent mechanisms activated in a dose-dependent manner. (A) MLH1-deficient HCT116+ch2 (open bars) and matched MMR-proficient HCT116+ch3 (filled bars) cells were treated with the indicated dose of MNNG, harvested 48 h after drug, fixed, stained with propidium iodide, and analyzed for cell cycle arrest by flow cytometry. Graphed is the percentage of cells within the analyzed population containing a 4N DNA content (G<sub>2</sub>/M fraction). (B) Isogenic ATM-deficient (EBS-7; open bars) and ATM-proficient (YZ-5; filled bars) cells were treated with indicated doses of MNNG and analyzed for cell cycle arrest as outlined in A. In each case, graphed is the average of five to eight independent experiments; error bar, SD.

Thus, we conclude from these findings that checkpoint response is dose dependent and that high MNNG-induced lesion loads activate a MMR-independent checkpoint response.

A parallel study on the ATM-deficient, SV40-transformed fibroblast line EBS-7 and isogenic ATM-proficient YZ-5 line also was conducted (Figure 2B). Here, we observed that neither line activated the G<sub>2</sub>/M checkpoint in response to 200 nM MNNG. In YZ-5 cells, we observed that exposure to 1  $\mu$ M MNNG resulted in a partial checkpoint response (<75% of the cells in G<sub>2</sub>/M 48 h after drug) but that moderate- (5 and 10  $\mu$ M) and high-dose (25  $\mu$ M) MNNG exposure fully activated checkpoint response in these cells. A dissimilar response to various doses of MNNG was observed in ATM-deficient EBS-7 cells. In these cells, like YZ-5, we found 200 nM MNNG did not activate a checkpoint response and that 1  $\mu$ M MNNG activated a suboptimal G<sub>2</sub>/M arrest. In clear contrast to ATM-proficient YZ-5 cells, however, we observed that EBS-7 cells exposed to 5 or 10  $\mu$ M MNNG displayed a blunted G<sub>2</sub>/M checkpoint response. At high dose (25  $\mu$ M MNNG), EBS-7 cells displayed a clear G<sub>2</sub>/M checkpoint response 48 h after drug. Together, these

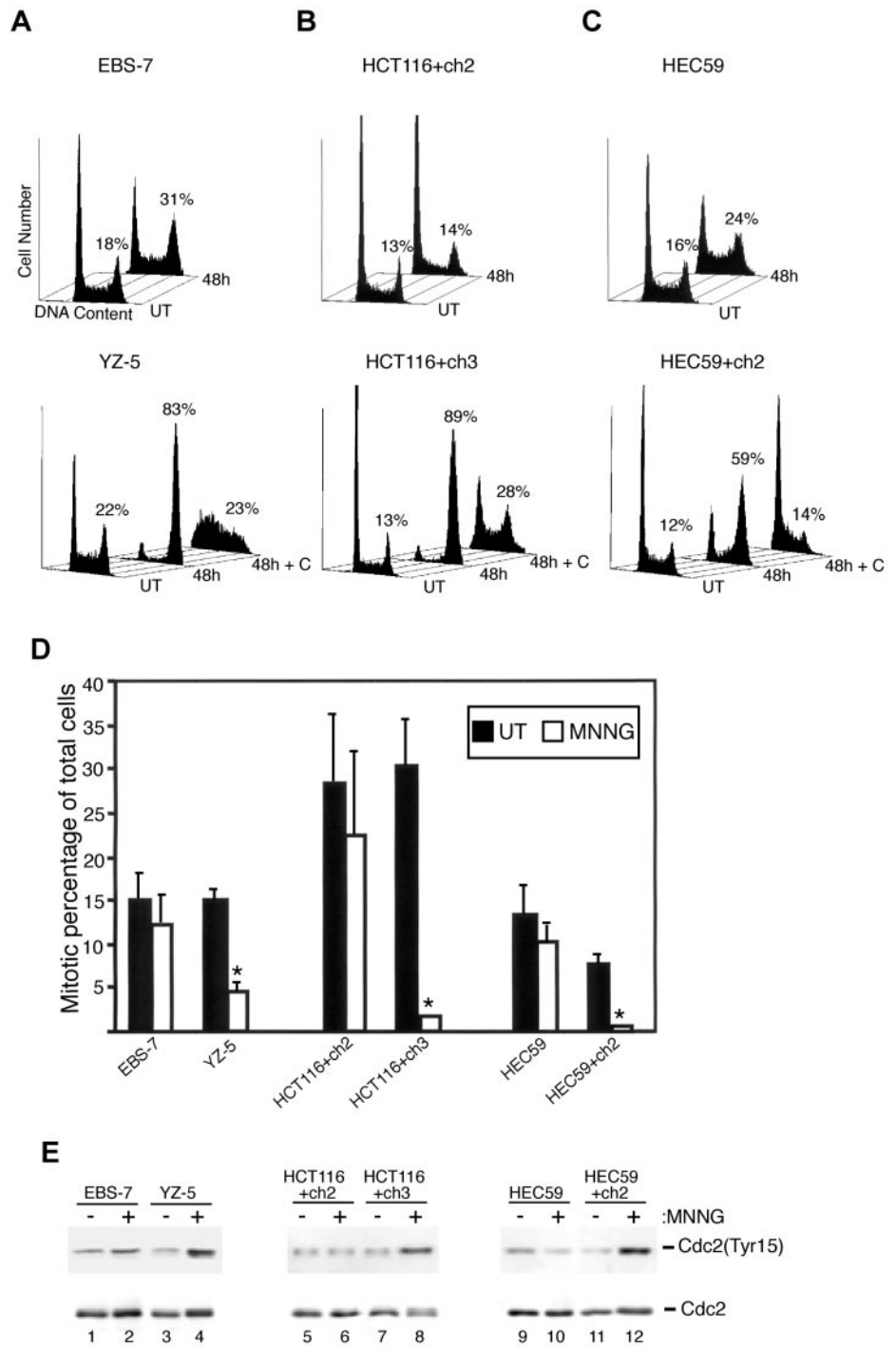


**Figure 3.** ATM and MMR are required for MNNG-induced G<sub>2</sub> arrest. (A) EBS-7 (top) and YZ-5 (bottom) cells were treated with 5 μM MNNG, and cells were harvested 48 h later and along with cultures of untreated (UT) logarithmically growing cells were fixed, stained with propidium iodide, and analyzed by flow cytometry. In addition, YZ-5 cells were treated with 5 mM caffeine (+C) before, during, and after MNNG exposure. The percentage of cells containing a 4N DNA content is noted. (B) MMR-deficient HCT116+ch2 (top) and isogenic MMR-proficient HCT116+ch3 (bottom) were treated with 5 μM MNNG with or without caffeine (+C) pretreatment, harvested 48 h after exposure, and analyzed by flow cytometry. (C) MMR-deficient HEC59 (top) and isogenic MMR-proficient HEC59+ch2 (bottom) were treated with 25 μM MNNG with or without caffeine (+C) pretreatment, harvested 48 h after exposure, and analyzed by flow cytometry. (D) EBS-7, YZ-5, HCT116+ch2, HCT116+ch3, HEC59, and HEC59+ch2 cells were either mock treated (open bars) or treated (filled bars) with MNNG and 48 h after drug, 0.4 μg/ml demecolcine was added to the medium. After a 24-h incubation, cells were fixed and stained for DNA and phosphohistone H3. Percentage of the total population of cells that progressed into mitosis during this time interval is graphed. The mean of three independent experiments is shown; error bars, 1 SD. Asterisk (\*) denotes  $p \leq 0.001$  (Student's *t*-test, two-tailed). (E) EBS-7 (lanes 1 and 2), YZ-5 (lanes 3 and 4), HCT116+ch2 (lanes 5 and 6), HCT116+ch3 (lanes 7 and 8), HEC59 (lanes 9 and 10), and HEC59+ch2 (lanes 11 and 12) cells were either mock treated (-) or treated with MNNG (+) and 48 h after drug exposure, cells were harvested, and lysates were formed and subjected to immunoblot analysis with antibodies against phospho-Tyr15 Cdc2 (top) or total Cdc2 (bottom).

observations indicate that MNNG triggers G<sub>2</sub>/M checkpoint response through dose-dependent activation of ATM-dependent and -independent pathway(s).

Next, we more fully documented the blunted G<sub>2</sub>/M checkpoint response in ATM-deficient fibroblasts. As outlined above, in response to 5 μM MNNG treatment, we observed that the ATM-complemented YZ-5 cells accumulate in G<sub>2</sub>/M 48 h after drug exposure. However, the isogenic ATM-deficient EBS-7 line clearly showed reduced G<sub>2</sub>/M accumulation at this time point in response to 5 μM MNNG treatment (Figure 3A). Specifically, we observed that

77.0 ± 9.9% (mean ± SD, n = 8) of 5 μM MNNG-treated YZ-5 cells display a 4N DNA content 48 h postdrug, indicating a robust checkpoint response. In contrast, 39.6 ± 8.8% (n = 7) of equivalently treated EBS-7 cells display a 4N DNA content at this time point, indicative of a blunted G<sub>2</sub>/M arrest. We conclude that ATM deficiency has a striking effect on the activation of G<sub>2</sub>/M arrest in response to MNNG because statistical analysis (Student's *t*-test, two-tailed) indicated a highly significant difference between the percentage of YZ-5 and EBS-7 cells in G<sub>2</sub> 48 h after 5 μM MNNG exposure ( $p = 3.1 \times 10^{-6}$ ). Furthermore, we have tested

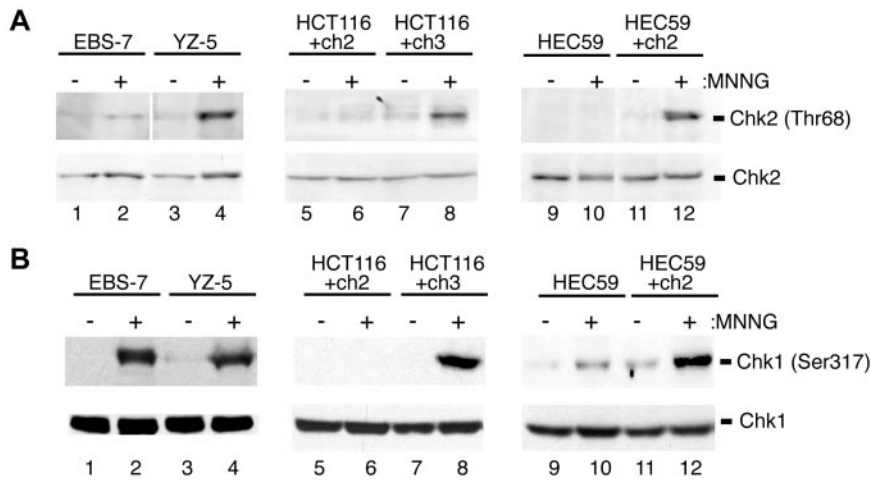


**Figure 4.** Requirement for MMR and ATM in MNNG-induced activation of Chk1 and Chk2. (A) EBS-7 (lanes 1 and 2), YZ-5 (lanes 3 and 4), HCT116+ch2 (lanes 5 and 6), HCT116+ch3 (lanes 7 and 8), HEC59 (lanes 9 and 10), and HEC59+ch2 (lanes 11 and 12) were either mock treated (-) or treated with MNNG (+) (5  $\mu$ M for EBS7/YZ-5, HCT116+ch2/HCT116+ch3; 25  $\mu$ M for HEC59/HEC59+ch2). Forty-eight hours after drug, lysates were formed and subjected to immunoblot analysis with antibodies against phospho-Thr68 Chk2 (top) or total Chk2 (bottom). (B) Lysates outlined above were immunoblotted with anti-phospho Ser317 Chk1 (top) or anti-total Chk1 (bottom).

numerous other transformed and nontransformed A-T-cell lines and found all lines examined show defective activation of  $G_2$  arrest in response to 5  $\mu$ M MNNG compared with normal lines (our unpublished data). Consistent with previous reports, we observed no MNNG-induced cell cycle arrest in the MLH1-deficient HCT116+ch2 cells treated with 5  $\mu$ M MNNG. However, MMR-complemented HCT116+ch3 cells showed prominent cell cycle arrest 48 h after drug addition (Figure 3B). MMR-dependent  $G_2$  arrest also was observed in MSH2-deficient HEC59 and MSH2-proficient HEC59+ch2 cells 48 h after 25  $\mu$ M MNNG exposure (Figure 3C) but not after 5  $\mu$ M MNNG (our unpublished data). We are currently unsure why HEC59+ch2 require higher doses of MNNG to activate  $G_2$ /M arrest, but this is likely attributable to the approximately fivefold higher MGMT expression that we have documented in this line compared with HCT116+ch3 cells (our unpublished data).

Caffeine is a potent inhibitor of ATM as well as structurally and functionally related PIK-like protein kinases such as ATR (Sarkaria *et al.*, 1999). We pretreated YZ-5, HCT116+ch3, and HEC59+ch2 cells with 5 mM caffeine before and after MNNG exposure (Figure 3, A–C, respectively). We observed that caffeine treatment abrogated MNNG-induced accumulation of cells with a 4N DNA content. These findings firmly underscore the role that PIK-like kinases play in establishing  $G_2$ /M arrest in response to MNNG.

To independently confirm these findings and ensure that MNNG was not inducing a general shutdown of cell growth in ATM- and MMR-deficient lines, we subjected these lines to the cytometry-based  $G_2$  checkpoint assay (Figure 1B). We observed that MNNG treatment resulted in a slight reduction of mitotic advance in EBS-7 cells; however, a significant  $G_2$  blockade was observed in YZ-5 cells treated in parallel (Figure 3D). Similarly, both MMR-deficient cell lines were unable to halt cell cycle advance after MNNG, whereas matched MMR-proficient lines effectively inhibited progression into mitosis.

Immunoblot analysis of EBS-7 cell lysates with anti-phospho Tyr15 antibody revealed only a slight increase in Cdc2 phosphorylation 48 h after drug; however, a clear accumulation of inactive Cdc2 was noted in YZ-5 cells after 5  $\mu$ M MNNG exposure (Figure 3E). Examination of MMR-deficient/proficient lines also indicates that accumulation of inactive Cdc2 after MNNG exposure is MMR dependent. In sum, these results clearly indicate that ATM deficiency re-

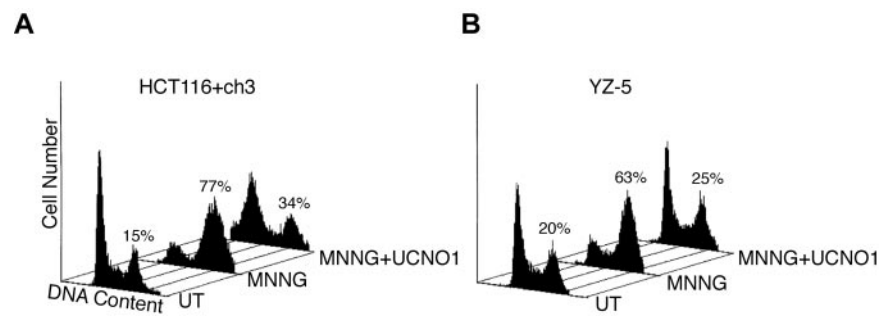
sults in a significant attenuation in establishment of this checkpoint in response to moderate MNNG doses.

#### *Chk1 Activation Requires the MMR System, whereas Chk2 Activation Requires Both ATM and MMR after Exposure to a Moderate Dose of MNNG*

We recently reported that Chk2 phosphorylation/activation, in response to low-dose gamma-irradiation, is both an ATM- and MMR-dependent process (Brown *et al.*, 2003). To determine whether MNNG-induced Chk2 activation has similar requirements, we exposed ATM-proficient/deficient and MMR-proficient/deficient lines to moderate doses of MNNG and assayed Chk2 phosphorylation at the time of maximal cell cycle arrest (48 h postdrug). We found that ATM-deficient EBS-7 cells treated with 5  $\mu$ M MNNG showed no increase in Thr68 phosphorylation after drug exposure (Figure 4A). Conversely, isogenic ATM-proficient YZ-5 fibroblasts displayed clear Thr68 phosphorylation 48 h after MNNG. Likewise, the MLH1-deficient line HCT116+ch2 did not display Chk2 Thr68 phosphorylation 48 h after 5  $\mu$ M MNNG treatment, whereas the matched MMR-proficient HCT116+ch3 line showed notable phosphorylation of this protein. We also assayed the MSH2-deficient line HEC59 and the matched MSH2-reconstituted line HEC59+ch2. Similar to the flow cytometry results outlined above, we found that 5  $\mu$ M MNNG failed to elicit a Chk2 phosphorylation response in either line at the 48-h time point (our unpublished data). However, when cells were treated with 25  $\mu$ M MNNG and harvested 48 h after drug, we observed robust Thr68 phosphorylation in MMR-proficient HEC59+ch2 but only minimal Chk2 phosphorylation in HEC59.

We next examined MNNG-induced phosphorylation of the Chk1 kinase. We found that, at MNNG doses that induce ATM-dependent phosphorylation of Chk2, Chk1 Ser317 phosphorylation was evident in the ATM-deficient EBS-7 cells as well as the ATM-proficient YZ-5 line (Figure 4B). In contrast, HCT116+ch2 cells displayed no Chk1 phosphorylation in response to 5  $\mu$ M MNNG, unlike MMR-proficient HCT116+ch3 cells. Similarly, MMR-deficient HEC59 cells displayed a notable reduction in Ser317 phosphorylation compared with MMR-proficient HEC59+ch2 cells. Together, these findings indicate that, in response to a moderate dose of MNNG, both Chk1 and Chk2 activation are MMR dependent, whereas Chk2 activation also requires ATM.

**Figure 5.** UCN-01 ablates MNNG-induced  $G_2$  arrest. (A) HCT116+ch3 cells were pretreated with 500 nM UCN-01 for 45 min before 5  $\mu$ M MNNG exposure, and UCN-01 was maintained in the culture medium during and after MNNG treatment. Mock treated (UT), MNNG-only treated, and MNNG/UCN-01-treated cells were harvested 48 h after MNNG exposure, fixed, stained with propidium iodide, and analyzed by flow cytometry. The percentage of cells containing a 4N DNA content is indicated. (B) YZ-5 cells were treated and analyzed as outlined in A. Percentage of cell population containing a 4N DNA content is given.



### Both Chk1 and Chk2 Are Necessary to Fully Activate MNNG-induced $G_2$ Arrest

Our findings that Chk1 and Chk2 activation occur in an MMR-dependent manner clearly suggested that activation of both kinases is required to establish  $G_2$  arrest after exposure to 5  $\mu$ M MNNG in HCT116+ch3 cells. To test this notion, we used the compound UCN-01, a potent inhibitor of Chk1 (Graves *et al.*, 2000). Furthermore, this compound has recently been shown to inhibit the catalytic activity of Chk2 as well (Yu *et al.*, 2002). YZ-5 or HCT116+ch3 cells were pretreated with 500 nM UCN-01 for 45 min before 5  $\mu$ M MNNG exposure, and UCN-01 was maintained in the culture medium during and after MNNG treatment. Cells were harvested 48 h after genotoxin, stained with propidium iodide, and analyzed by flow cytometry. We found that under these conditions that UCN-01 completely abrogated MNNG-induced  $G_2$  arrest in both YZ-5 (Figure 5A) and HCT116+ch3 (Figure 5B) cells.

Next, we tested the requirement for Chk1 and Chk2 in activating MNNG-induced  $G_2$  arrest by using RNAi to reduce their expression in HCT116+ch3 cells. As judged by immunoblotting, HCT116+ch3 cells transfected with commercially available (Dharmacon), pooled Chk1-specific siRNA duplexes displayed an approximate fivefold reduction in Chk1 expression compared with untransfected cells or cells transfected with siRNA duplexes specific for luciferase (Figure 6A, top). We found that Chk2 and control siRNA exerted no effect of Chk1 expression in these cells (Figure 6A, middle). Furthermore, we observed that mock-transfected cells (no siRNA included in transfection) or cells transfected with luciferase siRNA showed robust  $G_2$  arrest in response to 5  $\mu$ M MNNG (Figure 6B). In contrast, HCT116+ch3 cells transfected with Chk1-specific siRNA showed an approximate twofold reduction in the  $G_2$  cell population 48 h after MNNG treatment.

We also used this approach to knock down Chk2 expression in HCT116+ch3 cells. We observed that these cells, when transfected with commercially available, pooled Chk2 siRNA duplexes, displayed an approximately fourfold decrease in Chk2 abundance (Figure 6C, top). No effect on Chk1 expression was observed in cells transfected with Chk2 siRNA (Figure 6C, middle). Similar to results obtained using Chk1 siRNA, we observed an approximate twofold decrease in the  $G_2$  cell population in MNNG-treated cells transfected with Chk2 siRNA compared with mock-transfected or luciferase siRNA transfected cells (Figure 6D).

To independently confirm the results obtained using synthetic siRNA duplexes, we transfected cells with plasmids encoding either Chk1 (pKD-CHK1-v1) or Chk2 (pKD-CHK2-v3)-specific nucleotide sequences arranged to express shRNA molecules. The human H1 promoter (RNA pol III) drives the expression of these shRNA molecules that are

subsequently processed in the cell by endoribonucleases, thus forming an siRNA molecule (Paddison *et al.*, 2004). As a control, we used a plasmid (pKD-NegCon-v1) that encodes an shRNA with no homology to any gene in the human genome. HCT116+ch3 cells transfected with the Chk1 shRNA plasmid showed a marked decrease in Chk1 abundance after a 72-h transfection period but showed no decrease in Chk2 abundance (Figure 6E, top). Conversely, cells transfected with the Chk2 shRNA plasmid showed diminished Chk2 expression but no effects on Chk1 abundance were observed (Figure 6E, middle). When cells were cotransfected with both Chk1 and Chk2 shRNA plasmids, we observed decreased expression of both targeted proteins.

When transfected cells were treated with 5  $\mu$ M MNNG and analyzed by flow cytometry 48 h after drug we observed a significant diminishment in  $G_2$  arrest in either Chk1 shRNA or Chk2 shRNA-transfected cells compared with mock-transfected or cells transfected with the control plasmid (Figure 6F). When cells cotransfected with both Chk1 and Chk2 shRNA plasmids were treated with 5  $\mu$ M MNNG, we observed no additional reduction in  $G_2$  arrest than what was observed with either Chk1 or Chk2 shRNA plasmids used individually.

To confirm these observations biochemically, mock-transfected or cells transfected with control, Chk1, Chk2, or Chk1 and Chk2 shRNA plasmids were either mock treated or treated with 5  $\mu$ M MNNG, harvested 48 h after drug, and lysates were formed. Subsequently, these lysates were analyzed for Tyr15-phosphorylated Cdc2 abundance by immunoblotting (Figure 6G). We observed notable accumulation of inactive Cdc2 in MNNG-treated mock and control plasmid-transfected cells. Significantly lower, but clearly detectable, levels of Tyr15-phosphorylated Cdc2 were observed in HCT116+ch3 cells transfected with Chk1, Chk2, or Chk1 and Chk2 shRNA plasmids. These results agree with the blunted  $G_2$  arrest observed by flow cytometry in cells expressing reduced levels of Chk1 or Chk2. Collectively, these observations strongly suggest that both Chk1 and Chk2 are required to fully establish  $G_2$  arrest in HCT116+ch3 cells in response to 5  $\mu$ M MNNG exposure.

### Cdc25C Nuclear Exclusion after MNNG Exposure Is Dependent upon MMR

After gamma-irradiation, Chk1 and/or Chk2 phosphorylate the phosphatases Cdc25A and Cdc25C (Matsuoka *et al.*, 1998; Chaturvedi *et al.*, 1999; Falck *et al.*, 2001). Phosphorylation of Cdc25A triggers ubiquitin-dependent degradation of Cdc25A and forms the molecular basis for the S-phase checkpoint (Mailand *et al.*, 2000; Falck *et al.*, 2002). Furthermore, recent evidence implicates Cdc25A degradation in the initiation of  $G_2$ /M checkpoint after IR (Mailand *et al.*, 2002; Zhao *et al.*, 2002; Xiao *et al.*, 2003). To determine whether

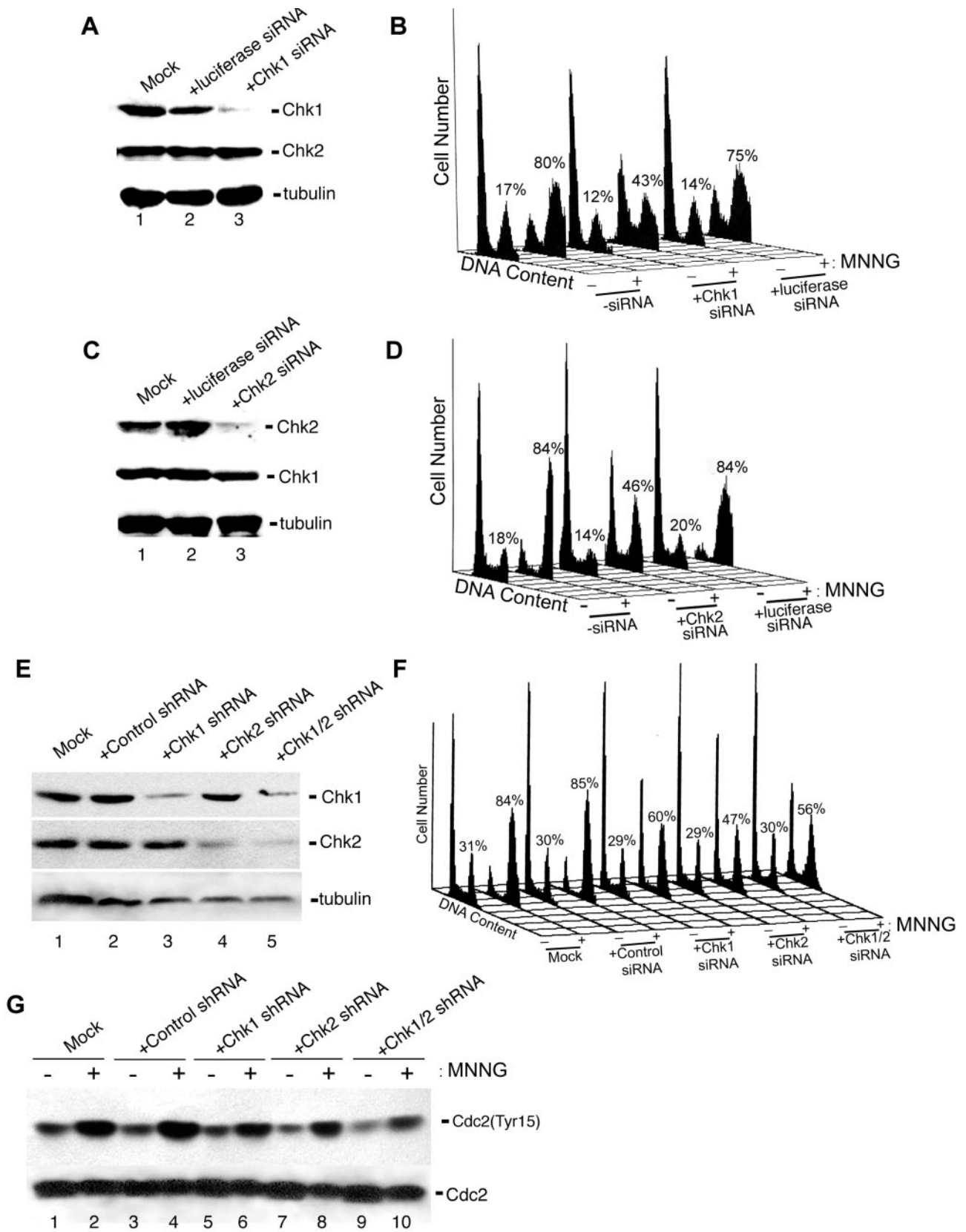
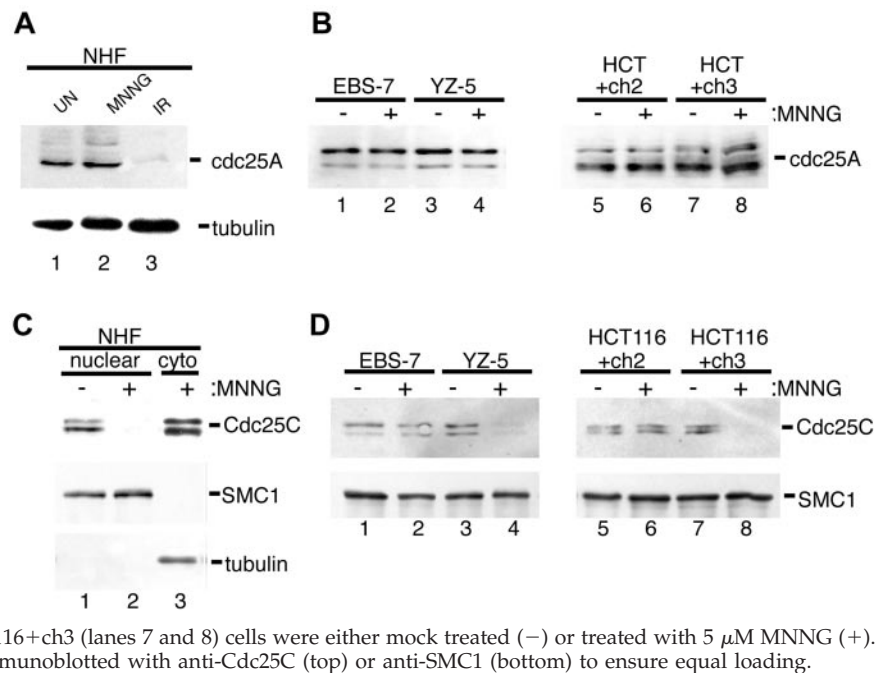


**Figure 6.** RNAi-induced depletion of Chk1 or Chk2 results in attenuation of the G<sub>2</sub> arrest activated by MNNG. (A) HCT116+ch3 cells were either mock transfected (no siRNA included in transfection, lane 1) or transfected with luciferase-specific siRNA (lane 2) or Chk1-specific siRNA (lane 3), and after transfection, cell extracts were immunoblotted with anti-total Chk1 (top), anti-total Chk2 (middle), or anti-tubulin (bottom) to confirm equivalent loading. (B) HCT116+ch3 cells were either mock-transfected or transfected with Chk1 or luciferase-specific



**Figure 7.** Nuclear exclusion of Cdc25C occurs in response to MNNG through an ATM- and MMR-dependent mechanism. (A) NHFs (lanes 1–3) were either mock treated (lane 1), 5  $\mu$ M MNNG treated (lane 2), or irradiated with 5 Gy of IR (lane 3). Cells were harvested 48 h after MNNG exposure or 1 h after irradiation, and total cell lysates were formed and subjected to immunoblot analysis with anti-Cdc25A (top) or tubulin (bottom). (B) ATM-deficient (lanes 1 and 2) and ATM-proficient (lanes 3 and 4) as well as MMR-deficient (lanes 5 and 6) and MMR-proficient (lanes 7 and 8) cells were either mock treated (lanes 1, 3, 5, and 7) or 5  $\mu$ M MNNG treated (lanes 2, 4, 6, and 8), total cell lysates were prepared 48 h after drug, and Cdc25A abundance was assessed by immunoblotting. (C) NHFs were either mock treated (lane 1) or treated with 5  $\mu$ M MNNG (lanes 2 and 3). Cells were fractionated into nuclear (lanes 1 and 2) or cytoplasmic (lane 3) components and immunoblotted with anti-Cdc25C (top), SMC1 (middle; nuclear fraction control), or tubulin (bottom; cytoplasmic fraction control). (D) EBS-7 (lanes 1 and 2), YZ-5 (lanes 3 and 4), HCT116+ch2 (lanes 5 and 6), and HCT116+ch3 (lanes 7 and 8) cells were either mock treated (–) or treated with 5  $\mu$ M MNNG (+). Nuclei were isolated 48 h after MNNG and immunoblotted with anti-Cdc25C (top) or anti-SMC1 (bottom) to ensure equal loading.



degradation of Cdc25A also plays a role in MNNG-induced G<sub>2</sub> arrest, we assayed Cdc25A abundance in NHFs after MNNG treatment. We observed no decrease in Cdc25A levels in the MNNG-treated cells 48 h after drug, but we did observe a prominent decrease in Cdc25A abundance 2 h after 10 Gy of IR (Figure 7A). Similar to NHFs, we did not observe any decrease in Cdc25A levels in either EBS-7/YZ-5 or HCT116+ch2/ch3 lines 48 h after 5  $\mu$ M MNNG exposure

(Figure 7B). It is possible that Cdc25A degradation plays a role in establishing G<sub>2</sub> arrest in response to MNNG at a time point before 48 h; however, these findings indicate that at the point of peak cell cycle arrest Cdc25A degradation does not correlate with G<sub>2</sub> arrest triggered by moderate doses of MNNG.

The phosphatase Cdc25C controls advance into mitosis by dephosphorylating and hence activating the cyclin-dependent kinase Cdc2. In response to gamma-irradiation, Chk1 and Chk2 phosphorylate Cdc25C on residue Ser216, triggering binding of Cdc25C to 14-3-3 proteins that, in turn, induce down-regulation of Cdc25C activity by promoting sequestration of the phosphatase from the nucleus to the cytoplasm. Analysis of fractionated NHFs revealed a dramatic drop in nuclear Cdc25C levels in MNNG-treated NHFs 48 h after MNNG treatment (Figure 7C). Similar experiments were carried out on isolated nuclei from MNNG-treated EBS-7/YZ-5 and HCT116+ch2/HCT116+ch3 cells (Figure 7D). We observed slight diminution in nuclear Cdc25C levels in ATM-deficient EBS-7 cells, but isogenic YZ-5 cells showed a marked reduction in nuclear Cdc25C abundance after MNNG. We observed a notable reduction in nuclear Cdc25C levels in MNNG-treated HCT116+ch3 cells, but no decrease in the nuclear levels of this protein were observed in drug-treated HCT116+ch2 cells. These experiments firmly indicate that, at the time of maximal MNNG-induced G<sub>2</sub> arrest, levels of Cdc25C within the nucleus diminish, and demonstrate the MMR-dependent nature of this event. Furthermore, the partial drop in nuclear Cdc25C abundance observed in the ATM-deficient EBS-7 line corresponds to the blunted G<sub>2</sub> checkpoint response observed in these cells when treated with moderate concentrations of MNNG.

#### MNNG Enhances the Association of Chk1 and Chk2 with the MMR Complex

We previously showed, using both in vivo and in vitro approaches, that Chk2 associates with the MMR protein MSH2 and that this interaction was enhanced in irradiated cells (Brown *et al.*, 2003). These findings led us to hypothe-

**Figure 6 (cont).** siRNA, treated with 5  $\mu$ M MNNG (+) or were mock treated (–), harvested 48 h later, and analyzed by flow cytometry. The percentage of cells containing a 4N DNA content is indicated. (C) HCT116+ch3 cells were either mock transfected (lane 1) or transfected with luciferase-specific siRNA (lane 2) or Chk2-specific siRNA (lane 3). After transfection, cell extracts were immunoblotted with anti-total Chk2 (top), anti-total Chk1 (middle), or anti-tubulin (bottom). (D) HCT116+ch3 cells were either mock transfected or transfected with Chk1 or luciferase-specific siRNA, exposed to 5  $\mu$ M MNNG (+) or mock treated (–), harvested 48 h later, and analyzed by flow cytometry. (E) HCT116+ch3 cells were either mock transfected (lane 1), transfected with the control shRNA plasmid pKD-NegCon-v1 (lane 2), the Chk1 shRNA plasmid pKD-CHK1-v1 (lane 3), the Chk2 shRNA plasmid pKD-CHK2-v3 (lane 4), or cotransfected with both CHK1 shRNA and CHK2 shRNA plasmids (lane 5) for 72 h. After this, cells were harvested and extracts were immunoblotted with anti-total Chk1 (top), anti-total Chk2 (middle), or anti-tubulin (bottom). (F) HCT116+ch3 cells were either mock transfected or transfected with indicated shRNA plasmids for 72 h. After transfection, cells were either treated with 5  $\mu$ M MNNG (+) or were mock treated (–), and 48 h later were analyzed by flow cytometry. The percentage of cells containing a 4N DNA content is indicated. (G) HCT116+ch3 cells were either mock transfected (lanes 1 and 2), transfected with the control shRNA plasmid pKD-NegCon-v1 (lanes 3 and 4), the Chk1 shRNA plasmid pKD-CHK1-v1 (lanes 5 and 6), the Chk2 shRNA plasmid pKD-CHK2-v3 (lanes 7 and 8), or cotransfected with both CHK1 shRNA and CHK2 shRNA plasmids (lanes 9 and 10) for 72 h. Subsequently, cells were either treated were mock treated (lanes 1, 3, 5, 7, and 9) or treated with 5  $\mu$ M MNNG (lanes 2, 4, 6, 8, and 10), and after a 48-h incubation, cells were harvested and extracts immunoblotted with antibodies against phospho-Tyr15 Cdc2 (top) or total Cdc2 (bottom).

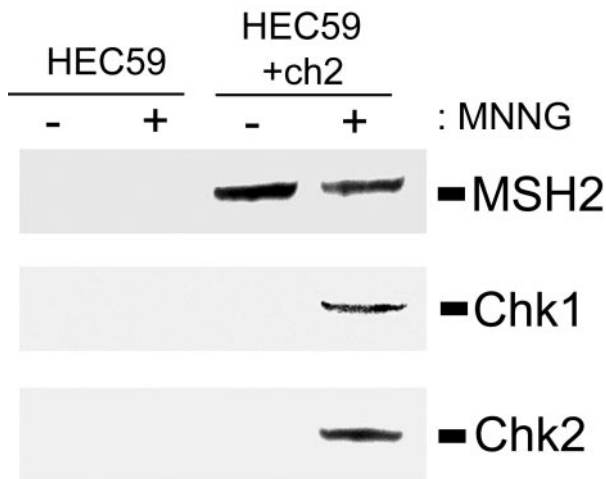


**Figure 8.** Chk1 and Chk2 coprecipitate with the MMR protein MSH2. MSH2-deficient HEC59 (lanes 1 and 2) and MSH2-proficient HEC59+ch2 (lanes 3 and 4) cells were either mock treated (lanes 1 and 3) or treated with 25  $\mu$ M MNNG (lanes 2 and 4) for 1 h. After a 48-h incubation cells were harvested, and extracts were formed and MSH2 was immunoprecipitated. The resultant immunocomplexes were subjected to immunoblot analysis with anti-MSH2 (top), anti-total Chk1 (middle), or anti-total Chk2 (bottom).

size that MMR complexes assembled at the sites of DNA damage formed a macromolecular scaffold that facilitated activation of Chk2. To test whether this damage-enhanced interaction also occurred after MNNG-induced DNA alkylation and whether this mechanism also may apply to Chk1 as well, we formed extracts from untreated and MNNG-treated (25  $\mu$ M) MSH2-deficient HEC59 and MSH2-proficient HEC59+ch2 cells. Subsequently, MSH2 was immunoprecipitated and the resultant immunocomplexes were analyzed by immunoblotting for coprecipitation of Chk2 or Chk1. We found that, as expected, no MSH2 was expressed in HEC59 cells but this protein was readily precipitated from HEC59+ch2 cell extracts (Figure 8, top). When MSH2 immunoprecipitations were immunoblotted with either anti-Chk1 (Figure 8, middle) or anti-Chk2 (Figure 8, bottom), we observed that these proteins coprecipitated with MSH2 in MNNG-treated cells. Longer exposures showed that both Chk1 and Chk2 associated with MSH2 in untreated cell extracts as well (our unpublished data). The requirement for MSH2 interaction is reinforced by the failure of either Chk1 or Chk2 to precipitate from HEC59 extracts. In sum, these findings indicate that both Chk1 and Chk2 associate, either directly or indirectly, with the MMR protein MSH2 and that this interaction is enhanced after MNNG-induced DNA alkylation.

## DISCUSSION

The focus of this study was to understand the mechanism(s) responsible for activation of the  $G_2/M$  checkpoint in response to the DNA methylator MNNG and the checkpoint pathway(s) defective in MMR-deficient cells. MMR mutants have long been known to fail to trigger  $G_2/M$  arrest in response to this and similar alkylators (Goldmacher *et al.*, 1986; Kat *et al.*, 1993; Koi *et al.*, 1994). We document that MNNG triggers  $G_2$  arrest through a mechanism that results in nuclear exclusion of Cdc25C and consequential accumulation of inactive Cdc2. Thus, the mechanism of  $G_2$  arrest in

response to MNNG uses evolutionarily conserved pathways common to other genotoxic agents (Strausfeld *et al.*, 1991; Lee *et al.*, 1992; Peng *et al.*, 1997; Dalal *et al.*, 1999). We also document that MMR-deficient cells fail to inactivate Cdc25C and Cdc2 in response to moderate doses of MNNG. Inactivation of these molecules and consequential  $G_2$  arrest correlate with activation of Chk1 and Chk2, and activation of both of these checkpoint kinases in response to moderate doses of MNNG requires MMR. Thus, we conclude that faulty activation of Chk1 and Chk2 is linked to the  $G_2/M$  checkpoint defect previously observed in MMR-deficient cells. Further study is required to determine whether defective activation of Chk1 and Chk2 also underlie other damage response defects that give rise to the alkylation-tolerant phenotype associated with MMR deficiency.

Chk1 and Chk2 are structurally dissimilar, but functionally related, protein kinases activated in response to DNA damage. Both Chk1 and Chk2 phosphorylate Cdc25C *in vitro* (Sanchez *et al.*, 1997; Matsuoka *et al.*, 1998; Brown *et al.*, 1999); thus, such overlap in function suggests that these molecules serve redundant roles in establishing  $G_2$  arrest in response to genotoxic insult. However, current evidence indicates that IR-induced  $G_2$  arrest is Chk1 dependent and that Chk2 is not required to activate this checkpoint in response to IR (Liu *et al.*, 2000). In contrast, by using an RNAi approach, we observed that reduced Chk2 expression partially suppressed MNNG-induced  $G_2$  arrest. Furthermore, we document that Chk2 activation in response to moderate doses of MNNG is ATM-dependent and that ATM-deficient cells exhibit a blunted checkpoint response to moderate doses of MNNG. Thus, these findings seemingly support a key role for Chk2 in response to moderate doses MNNG.

We also document that reduced Chk1 expression resulted in a blunted checkpoint response after moderate doses of MNNG, and activation of Chk1 at this MNNG concentration is dependent upon MMR. This result is in agreement with the observations of Wang and Qin (2003) who showed, by using RNAi methodology, that reduced MSH2 expression resulted in defects in Chk1 activation after exposure of HeLa cells to 10  $\mu$ M MNNG. Together, we conclude that in addition to MMR-dependent activation of Chk2, MMR-dependent Chk1 activation plays a fundamental role during activation of the  $G_2$  checkpoint in response to moderate doses of MNNG.

Our findings indicate that both Chk1 and Chk2 are required for optimal activation of the  $G_2$  checkpoint in response to moderate doses of MNNG. This outcome may well indicate that these kinases work in an additive manner to activate this checkpoint through Cdc25C and Cdc2 inactivation. However, we also observed that reduced expression of both Chk1 and Chk2 resulted in no apparent additional diminishment of arrest compared with cells with individual knockdown of Chk1 or Chk2 expression. This result could be attributable to residual Chk1 and/or Chk2 expression in cells subjected to RNAi or may suggest that these kinases function at different points in the same checkpoint pathway. Alternatively, other checkpoint pathway(s) may be activated by Chk1 or Chk2 and, without the action of both kinases and their associated downstream signaling mechanisms, such alternate pathways cannot optimally establish  $G_2$  arrest. Although both Chk1 and Chk2 have the potential to inhibit Cdc25C activity, and Cdc25C is clearly targeted for inactivation by  $G_2/M$  checkpoint pathways, increases in kinase activity that promote inhibitory phosphorylation of Cdc2 also would result in a blockade to mitotic entry. At present, Wee1 and Myt1 are the character-

ized kinases capable of phosphorylating the Tyr15 residue of Cdc2. In yeast, the Myt1 homolog (termed Mik1) is rapidly up-regulated in response to either hydroxyurea-induced replication arrest (Boddy *et al.*, 1998) or ionizing radiation (Christensen *et al.*, 2000). Furthermore, Christensen and colleagues found, depending upon the phase of the cell cycle the cells are in when irradiated, that Mik1 up-regulation was dependent upon the yeast homolog of Chk2 (termed Cds1) or Chk1. Because Mik1 is a dose-dependent inhibitor of mitotic entry in both yeast (Lundgren *et al.*, 1991) and mammalian cells (Liu *et al.*, 1999) and has been proposed to be a component in DNA damage-activated checkpoints in yeast (Baber-Furnari *et al.*, 2000; Christensen *et al.*, 2000), it is plausible that Myt1 may perform a similar checkpoint function in mammalian cells. However, a role for Myt1 in mammalian DNA damage response is currently unresolved.

It also is possible that checkpoint pathways, other than those that function through inhibiting Cdc25 and Cdc2 activity, are activated in response to MNNG-induced DNA damage. One such potential mechanism is control over localization of Cdc2 itself. Specifically, Cdc2 complexes with its regulatory subunit cyclin B to form maturation-promoting factor (MPF), and the catalytic action of MPF is required to propel cells from interphase into mitosis. MPF, which is exclusively cytoplasmic during interphase, must accumulate within the nucleus to promote events key to mitotic entry (e.g., nuclear envelope breakdown and chromatin condensation) (Ohi and Gould, 1999). The localization of MPF is tightly controlled by its rapid exclusion from the nucleus facilitated by the interaction of cyclin B with the nuclear export receptor CRM1 (Hagting *et al.*, 1998; Yang *et al.*, 1998). Phosphorylation of multiple serine residues within the N-terminal region of cyclin B inhibits CRM1/cyclin B interaction, resulting in nuclear retention of MPF and consequential promotion of mitotic onset (Yang *et al.*, 2001; Walsh *et al.*, 2003). Thus, it is possible that MNNG exposure triggers pathway(s) that interfere with the nuclear localization of MPF (or other required mitotic factors) by governing the activity of molecules such as CRM1 that are important in controlling the cellular machinery that promotes transition from G<sub>2</sub> to M phase. Certainly, much work lies ahead to more fully understand the mechanisms that control the G<sub>2</sub> checkpoint in response to genotoxins such as MNNG.

Cells lacking ATM show a defect in rapidly halting advance into mitosis after IR but are ultimately capable of activating an effective G<sub>2</sub> arrest. This led Xu *et al.* (2002) to conclude that there are at least two distinct G<sub>2</sub> checkpoint mechanisms activated in response to IR. The first is ATM dependent and is responsible for rapid establishment of a block to mitotic entry; the second is ATM independent and results in accumulation of cells in G<sub>2</sub>. In contrast, we found that ATM was required for optimal establishment of G<sub>2</sub> arrest in response to moderate doses of MNNG. To our knowledge, the findings described here are the first example of a requirement for ATM in triggering accumulation of G<sub>2</sub>-arrested cells in response to genotoxic insult.

We also document that caffeine abrogated MNNG-induced G<sub>2</sub> arrest and because caffeine has strong inhibitory effects on the ATM-related kinase ATR, it is likely that ATR is a necessary component in MNNG-induced checkpoint activation as well. Given that several studies indicate Chk1 is activated by ATR in response to a variety of genotoxins (Liu *et al.*, 2000), including MNNG (Wang and Qin, 2003; Beardsley and Brown, unpublished data), it is probable that ATR is responsible for the Chk1 activation documented in our study. Conversely, several groups have documented a requirement for ATM in Chk2 activation after gamma-irra-

diation (Matsuoka *et al.*, 1998; Chaturvedi *et al.*, 1999; Ahn *et al.*, 2000; Matsuoka *et al.*, 2000; Zhou *et al.*, 2000; Falck *et al.*, 2001). The data presented in this report agree with these studies because we observed that ATM-deficient cells fail to activate Chk2 in response to moderate doses of MNNG. Thus, we conclude that both ATM and ATR are activated in response to MNNG, that these kinases phosphorylate/activate Chk2 and Chk1, respectively, and that these signal transduction mechanisms are required for MNNG-induced G<sub>2</sub> arrest.

While this manuscript was in revision, Stojic *et al.* (2004) reported that low-dose (0.2  $\mu$ M) MNNG exposure resulted in an ATM-independent G<sub>2</sub> arrest in the isogenic ATM-proficient/deficient (YZ-5/EBS-7) fibroblast lines used in our study. Although this seems contrary to the findings reported here, notable differences in experimental approach exist between the two studies. Principally, in the study published by Stojic and colleagues both EBS-7 and YZ-5 cells were treated with O<sup>6</sup>-benzylguanine, an irreversible inhibitor of the DNA repair protein MGMT (Dolan *et al.*, 1990), before, during, and after MNNG treatment. Thus, although 0.2  $\mu$ M MNNG will produce a lower initial O<sup>6</sup>MeG lesion load than the drug concentrations used in this report, it is predictable that such mutagenic adducts will persist longer in these cells compared with cells with intact MGMT activity. The persistent nature of these lesions could, potentially, change the profile of MNNG-induced damage response similar to the dose-dependent ATM and MMR requirement for activation of G<sub>2</sub> arrest observed in cells treated with a range of MNNG concentrations (Figure 2). For example, we document that EBS-7/YZ-5 cells with intact MGMT activity treated with 0.2  $\mu$ M MNNG fail to elicit a G<sub>2</sub> checkpoint response and that high-dose (25  $\mu$ M) MNNG activates G<sub>2</sub> arrest in an ATM-independent manner. Furthermore, Stojic and coworkers documented that, under their treatment conditions, Cdc25A degradation correlated with G<sub>2</sub> checkpoint activation (48 h after drug), whereas we have documented no change in the cellular abundance of this protein at this time point in cells treated with 5  $\mu$ M MNNG in the absence of O<sup>6</sup>-benzylguanine. Also, under the outlined conditions, Stojic and coworkers observed that Chk2 activation occurred in an ATM-independent manner, whereas we have observed ATM-dependent Chk2 activation in response to 5  $\mu$ M MNNG without MGMT inhibition. Of note, Matsuoka *et al.* (2000) documented that IR induces ATM-dependent Chk2 phosphorylation, whereas an ATM-independent mechanism (presumably ATR) phosphorylates Chk2 in response to UV light or hydroxyurea. On balance, the distinct differences between the findings reported in the Stojic and coworkers study and the work outlined here strongly suggest that inhibition of MGMT can produce profound changes on cellular response to MNNG-induced DNA alkylation.

Collectively, our findings lead us to propose that MNNG-induced G<sub>2</sub> checkpoint response is governed by ATM- and ATR-dependent pathways, both of which are activated in a MMR-dependent manner. Although these pathways are activated in response to MNNG and are critical to the establishment of G<sub>2</sub> arrest, recent studies suggest that these may not be the only MMR-dependent pathways activated in response to DNA damage. Hirose *et al.* (2003) showed that, in response to temozolomide, catalytic activation of the kinase p38 $\alpha$  occurs through a MMR-dependent mechanism. Furthermore, blocking p38 $\alpha$  activity by pharmacological and RNAi approaches led to abrogation of temozolomide-induced G<sub>2</sub> arrest. Although loss of p38 $\alpha$  did not impact ATM-dependent phosphorylation of Chk2 (Thr68), these workers did observe diminished Cdc25C and Cdc2 phos-

phorylation when p38 $\alpha$  activity or abundance was reduced. This clearly suggests that p38 $\alpha$  is a component in the G<sub>2</sub> checkpoint machinery and functions through promoting inactivation of Cdc25C and Cdc2. Although it is unclear how p38 $\alpha$  functions in this pathway(s), others have presented evidence consistent with a role for the p38 $\gamma$  isoform in irradiation-induced Chk2 activation (Wang *et al.*, 2000). Whereas four isoforms of the p38 kinase have been identified to date, the exact nature of how these various forms of p38 function in damage-induced signaling is likely complicated.

Two nonmutually exclusive theories have been proposed to explain the link between MMR and cellular response to methylators such as MNNG. The first model attributes the cytotoxic effects of these genotoxins to MMR-dependent repair of O<sup>6</sup>MeG:T base pairs that arise after replication. These aberrant structures trigger cycles of futile repair by the MMR system, resulting in persistent excision intermediates within the genome, which, in turn, activate DNA damage response (Goldmacher *et al.*, 1986; Kat *et al.*, 1993). The second model holds that MMR repair proteins form a complex at a lesion site and, after doing so, play an active role in initiating signal transduction pathways (Duckett *et al.*, 1996; Mello *et al.*, 1996).

Save for our observation that MNNG-induced G<sub>2</sub> arrest is slow to occur, which is consistent with previous findings indicating that a round of DNA replication is required to trigger cell cycle arrest in response to this class of genotoxins (Plant and Roberts, 1971; Goldmacher *et al.*, 1986; Zhukovskaya *et al.*, 1994; Stojic *et al.*, 2004), the results of our study neither support nor disagree with the former model. However, our findings reinforce the validity of the latter MMR system/signaling complex hypothesis. We previously found that ATM and Chk2 associate with the MMR proteins MLH1 and MSH2, respectively (Brown *et al.*, 2003). This finding led us to hypothesize that MMR complexes formed at the sites of IR-induced lesions form a macromolecular scaffold that promotes ATM-dependent Chk2 activation. Here, we extend these earlier studies by demonstrating that both Chk1 and Chk2 associate with the MMR protein MSH2. Furthermore, these interactions are clearly enhanced in response to MNNG. When interpreted along with the data that O<sup>6</sup>MeG lesions are recognized by the MMR system (Griffin *et al.*, 1994; Duckett *et al.*, 1996, 1999) and that both Chk1 and Chk2 activation in response to MNNG is MMR dependent, it is tempting to speculate that association of Chk1 and Chk2 with MMR complexes assembled at the sites of DNA damage is required for their activation in response to moderate levels of MNNG-induced damage.

Additional lines of investigation further support an active, structural role for MMR complexes in DNA damage signaling. For example, ATR has recently been shown to associate with MSH2 to form a proposed "signaling module" required for activation of a subset of damage-induced pathways (Wang and Qin, 2003). Perhaps the most elegant studies in support of a potential structural role for MMR complexes in activation of damage signaling come from analysis of MSH2 mutants. Specifically, Lin *et al.* (2004) observed that mouse cells expressing mutant Msh2 with disrupted ATPase activity displayed normal Msh2 binding to damaged DNA and apoptotic response to cisplatin, but they were incapable of supporting DNA repair. Similar findings were obtained using yeast strains harboring a range of engineered mutations in the Msh2 ATPase domain (Drotschmann *et al.*, 2004). Because the MMR system is required to properly trigger apoptogenic signaling in response to cisplatin (Aebi *et al.*, 1996), these results plainly indicate that repair activity can

be uncoupled from DNA damage recognition and response signaling. Clearly, separation-of-function mutants that support DNA repair but not damage signaling are required to formally test our proposal that MMR complexes function as molecular scaffolds at the sites of DNA lesions to facilitate DNA damage signaling.

In conclusion, our findings help explain the molecular basis for abrogated methylator-induced G<sub>2</sub> arrest in MMR-deficient cells. The MMR system is targeted for inactivation in the cancer-predisposing syndrome hereditary nonpolyposis colorectal cancer (HNPCC) (Papadopoulos *et al.*, 1994). One of the hallmark features of HNPCC is heightened mutation rates, most notably increased microsatellite instability. Loss of DNA damage-induced cell cycle checkpoints will further exacerbate genomic instability and presumably raise the likelihood of cancer arising from inactivation of the MMR system.

## ACKNOWLEDGMENTS

We thank Dr. Thomas Kunkel (National Institute of Environmental Health Sciences) for the generous gift of HEC59 and HEC59+ch2 cells and Dr. Bo Xu (Department of Genetics, Louisiana State University Health Sciences Center) for technical advice. We also thank the monitoring editor of this manuscript, Dr. Tony Hunter, for keen insight, helpful criticisms, and unwavering patience during the revision process. This work was supported by grants from the American Cancer Society (GMC-99198) and National Institutes of Health (R01-CA102289) to K.D.B. A.W.A. and D.I.B. were supported, in part, by predoctoral fellowships from the Stanley S. Scott Cancer Center.

## REFERENCES

- Abraham, R. T. (2001). Cell cycle checkpoint signaling through the ATM and ATR kinases. *Genes Dev.* 15, 2177–2196.
- Adamson, A. W., Kim, W. J., Shangary, S., Baskaran, R., and Brown, K. D. (2002). ATM is activated in response to N-methyl-N'-nitro-N-nitrosoguanidine-induced DNA alkylation. *J. Biol. Chem.* 277, 38222–38229.
- Aebi, S., *et al.* (1996). Loss of DNA mismatch repair in acquired resistance to cisplatin. *Cancer Res.* 56, 3087–3090.
- Ahn, J. Y., Schwarz, J. K., Piwnica-Worms, H., and Canman, C. E. (2000). Threonine 68 phosphorylation by ataxia telangiectasia mutated is required for efficient activation of Chk2 in response to ionizing radiation. *Cancer Res.* 60, 5934–5936.
- Allen, D. M., *et al.* (2001). Ataxia telangiectasia mutated is essential during adult neurogenesis. *Genes Dev.* 15, 554–566.
- Baber-Furnari, B. A., Rhind, N., Boddy, M. N., Shanahan, P., Lopez-Girona, A., and Russell, P. (2000). Regulation of mitotic inhibitor mik1 helps to enforce the DNA damage checkpoint. *Mol. Biol. Cell* 11, 1–11.
- Bakkenist, C. J., and Kastan, M. B. (2003). DNA damage activates ATM through intermolecular autophosphorylation and dimer dissociation. *Nature* 421, 499–506.
- Boddy, M. N., Furnari, B., Mondesert, O., and Russell, P. (1998). Replication checkpoint enforced by kinases Cds1 and Chk1. *Science* 280, 909–912.
- Branch, P., Aquilina, G., Bignami, M., and Karran, P. (1993). Defective mismatch binding and a mutator phenotype in cells tolerant to DNA damage. *Nature* 362, 652–654.
- Brown, A. L., Lee, C. H., Schwarz, J. K., Mitiku, N., Piwnica-Worms, H., and Chung, J. H. (1999). A human Cds1-related kinase that functions downstream of ATM protein in the cellular response to DNA damage. *Proc. Natl. Acad. Sci. USA* 96, 3745–3750.
- Brown, K. D., Rathi, A., Kamath, R., Beardsley, D. I., Zhan, Q., Mannino, J. L., and Baskaran, R. (2003). The mismatch repair system is required for S-phase checkpoint activation. *Nat. Genet.* 33, 80–84.
- Cejka, P., Stojic, L., Mojas, N., Russell, A. M., Heinemann, K., Cannavo, E., di Pietro, M., Marra, G., and Jiricny, J. (2003). Methylation-induced G(2)/M arrest requires a full complement of the mismatch repair protein hMLH1. *EMBO J.* 22, 2245–2254.
- Chaturvedi, P., *et al.* (1999). Mammalian Chk2 is a downstream effector of the ATM-dependent DNA damage checkpoint pathway. *Oncogene* 18, 4047–4054.

- Christensen, P. U., Bentley, N. J., Martinho, R. G., Nielsen, O., and Carr, A. M. (2000). Mik1 levels accumulate in S phase and may mediate an intrinsic link between S phase and mitosis. *Proc. Natl. Acad. Sci. USA* *97*, 2579–2584.
- Cliby, W. A., Roberts, C. J., Cimprich, K. A., Stringer, C. M., Lamb, J. R., Schreiber, S. L., and Friend, S. H. (1998). Overexpression of a kinase-inactive ATR protein causes sensitivity to DNA-damaging agents and defects in cell cycle checkpoints. *EMBO J.* *17*, 159–169.
- Dalal, S. N., Schweitzer, C. M., Gan, J., and DeCaprio, J. A. (1999). Cytoplasmic localization of human cdc25C during interphase requires an intact 14-3-3 binding site. *Mol. Cell. Biol.* *19*, 4465–4479.
- Dolan, M. E., Moschel, R. C., and Pegg, A. E. (1990). Depletion of mammalian O6-alkylguanine-DNA alkyltransferase activity by O6-benzylguanine provides a means to evaluate the role of this protein in protection against carcinogenic and therapeutic alkylating agents. *Proc. Natl. Acad. Sci. USA* *87*, 5368–5372.
- Drotschmann, K., Topping, R. P., Clodfelter, J. E., and Salsbury, F. R. (2004). Mutations in the nucleotide-binding domain of MutS homologs uncouple cell death from cell survival. *DNA Repair* *3*, 729–742.
- Duckett, D. R., Bronstein, S. M., Taya, Y., and Modrich, P. (1999). hMutSalph and hMutLalpha-dependent phosphorylation of p53 in response to DNA methylator damage. *Proc. Natl. Acad. Sci. USA* *96*, 12384–12388.
- Duckett, D. R., Drummond, J. T., Murchie, A. I., Reardon, J. T., Sancar, A., Lilley, D. M., and Modrich, P. (1996). Human MutSalph recognizes damaged DNA base pairs containing O6-methylguanine, O4-methylthymine, or the cisplatin-d(GpG) adduct. *Proc. Natl. Acad. Sci. USA* *93*, 6443–6447.
- Falck, J., Mailand, N., Syljuasen, R. G., Bartek, J., and Lukas, J. (2001). The ATM-Chk2-Cdc25A checkpoint pathway guards against radioresistant DNA synthesis. *Nature* *410*, 842–847.
- Falck, J., Petrini, J. H., Williams, B. R., Lukas, J., and Bartek, J. (2002). The DNA damage-dependent intra-S phase checkpoint is regulated by parallel pathways. *Nat. Genet.* *30*, 290–294.
- Goldmacher, V. S., Cuzick, R. A., Jr., and Thilly, W. G. (1986). Isolation and partial characterization of human cell mutants differing in sensitivity to killing and mutation by methylnitrosourea and N-methyl-N'-nitro-N-nitrosoguanidine. *J. Biol. Chem.* *261*, 12462–12471.
- Graves, P. R., Yu, L., Schwarz, J. K., Gales, J., Sausville, E. A., O'Connor, P. M., and Piwnica-Worms, H. (2000). The Chk1 protein kinase and the Cdc25C regulatory pathways are targets of the anticancer agent UCN-01. *J. Biol. Chem.* *275*, 5600–5605.
- Griffin, S., Branch, P., Xu, Y. Z., and Karran, P. (1994). DNA mismatch binding and incision at modified guanine bases by extracts of mammalian cells: implications for tolerance to DNA methylation damage. *Biochemistry* *33*, 4787–4793.
- Hagting, A., Karlsson, C., Clute, P., Jackman, M., and Pines, J. (1998). MPP localization is controlled by nuclear export. *EMBO J.* *17*, 4127–4138.
- Hartwell, L. H., and Kastan, M. B. (1994). Cell cycle control and cancer. *Science* *266*, 1821–1828.
- Hirose, Y., Katayama, M., Stokoe, D., Haas-Kogan, D. A., Berger, M. S., and Pieper, R. O. (2003). The p38 mitogen-activated protein kinase pathway links the DNA mismatch repair system to the G2 checkpoint and to resistance to chemotherapeutic DNA-methylating agents. *Mol. Cell. Biol.* *23*, 8306–8315.
- Jaiswal, A. S., Multani, A. S., Pathak, S., and Narayan, S. (2004). N-Methyl-N'-nitro-N-nitrosoguanidine-induced senescence-like growth arrest in colon cancer cells is associated with loss of adenomatous polyposis coli protein, microtubule organization, and telomeric DNA. *Mol. Cancer* *3*, 3.
- Jallepalli, P. V., Lengauer, C., Vogelstein, B., and Bunz, F. (2003). The Chk2 tumor suppressor is not required for p53 responses in human cancer cells. *J. Biol. Chem.* *278*, 20475–20479.
- Kalamegham, R., Warmels-Rodenhiser, S., MacDonald, H., and Ebisuzaki, K. (1988). O6-Methylguanine-DNA methyltransferase-defective human cell mutant: O6-methylguanine, DNA strand breaks and cytotoxicity. *Carcinogenesis* *9*, 1749–1753.
- Karran, P., and Bignami, M. (1992). Self-destruction and tolerance in resistance of mammalian cells to alkylation damage. *Nucleic Acids Res.* *20*, 2933–2940.
- Kastan, M. B., Onyekwere, O., Sidransky, D., Vogelstein, B., and Craig, R. W. (1991). Participation of p53 protein in the cellular response to DNA damage. *Cancer Res.* *51*, 6304–6311.
- Kat, A., Thilly, W. G., Fang, W. H., Longley, M. J., Li, G. M., and Modrich, P. (1993). An alkylation-tolerant, mutator human cell line is deficient in strand-specific mismatch repair. *Proc. Natl. Acad. Sci. USA* *90*, 6424–6428.
- Kaufmann, W. K., and Wilson, S. J. (1994). G1 arrest and cell-cycle-dependent clastogenesis in UV-irradiated human fibroblasts. *Mutat. Res.* *314*, 67–76.
- Koi, M., Umar, A., Chauhan, D. P., Cherian, S. P., Carethers, J. M., Kunkel, T. A., and Boland, C. R. (1994). Human chromosome 3 corrects mismatch repair deficiency and microsatellite instability and reduces N-methyl-N'-nitro-N-nitrosoguanidine tolerance in colon tumor cells with homozygous hMLH1 mutation. *Cancer Res.* *54*, 4308–4312.
- Lee, M. S., Ogg, S., Xu, M., Parker, L. L., Donoghue, D. J., Maller, J. L., and Piwnica-Worms, H. (1992). cdc25+ encodes a protein phosphatase that dephosphorylates p34cdc2. *Mol. Biol. Cell* *3*, 73–84.
- Lin, D. P., et al. (2004). An Msh2 point mutation uncouples DNA mismatch repair and apoptosis. *Cancer Res.* *64*, 517–522.
- Lindahl, T., Demple, B., and Robins, P. (1982). Suicide inactivation of the E. coli O6-methylguanine-DNA methyltransferase. *EMBO J.* *1*, 1359–1363.
- Liu, F., Rothblum-Oviatt, C., Ryan, C. E., and Piwnica-Worms, H. (1999). Overproduction of human Myt1 kinase induces a G2 cell cycle delay by interfering with the intracellular trafficking of Cdc2-Cyclin B1 complexes. *Mol. Cell. Biol.* *19*, 5113–5123.
- Liu, Q., et al. (2000). Chk1 is an essential kinase that is regulated by Atr and required for the G(2)/M DNA damage checkpoint. *Genes Dev.* *14*, 1448–1459.
- Loeb, L. A., Loeb, K. R., and Anderson, J. P. (2003). Multiple mutations and cancer. *Proc. Natl. Acad. Sci. USA* *100*, 776–781.
- Lundgren, K., Walworth, N., Booher, R., Dembski, M., Kirschner, M., and Beach, D. (1991). mik1 and wee1 cooperate in the inhibitory tyrosine phosphorylation of cdc2. *Cell* *64*, 1111–1122.
- Mailand, N., Falck, J., Lukas, C., Syljuasen, R. G., Welcker, M., Bartek, J., and Lukas, J. (2000). Rapid destruction of human Cdc25A in response to DNA damage. *Science* *288*, 1425–1429.
- Mailand, N., Podtelejnikov, A. V., Groth, A., Mann, M., Bartek, J., and Lukas, J. (2002). Regulation of G(2)/M events by Cdc25A through phosphorylation-dependent modulation of its stability. *EMBO J.* *21*, 5911–5920.
- Matsuoka, S., Huang, M., and Elledge, S. J. (1998). Linkage of ATM to cell cycle regulation by the Chk2 protein kinase. *Science* *282*, 1893–1897.
- Matsuoka, S., Rotman, G., Ogawa, A., Shiloh, Y., Tamai, K., and Elledge, S. J. (2000). Ataxia telangiectasia-mutated phosphorylates Chk2 in vivo and in vitro. *Proc. Natl. Acad. Sci. USA* *97*, 10389–10394.
- Mello, J. A., Acharya, S., Fishel, R., and Essigmann, J. M. (1996). The mismatch-repair protein hMSH2 binds selectively to DNA adducts of the anticancer drug cisplatin. *Chem. Biol.* *3*, 579–589.
- Ohi, R., and Gould, K. L. (1999). Regulating the onset of mitosis. *Curr. Opin. Cell Biol.* *11*, 267–273.
- Paddison, P. J., Caudy, A. A., Sachidanandam, R., and Hannon, G. J. (2004). Short hairpin activated gene silencing in Mammalian cells. *Methods Mol. Biol.* *265*, 85–100.
- Papadopoulos, N., et al. (1994). Mutation of a mutL homolog in hereditary colon cancer. *Science* *263*, 1625–1629.
- Paules, R. S., Levedakou, E. N., Wilson, S. J., Innes, C. L., Rhodes, N., Tlsty, T. D., Galloway, D. A., Donehower, L. A., Tainsky, M. A., and Kauffmann, W. K. (1995). Defective G2 checkpoint function in cells from individuals with familial cancer syndromes. *Cancer Res.* *55*, 1763–1773.
- Peng, C. Y., Graves, P. R., Thoma, R. S., Wu, Z., Shaw, A. S., and Piwnica-Worms, H. (1997). Mitotic and G2 checkpoint control: regulation of 14–3–3 protein binding by phosphorylation of Cdc25C on serine-216. *Science* *277*, 1501–1505.
- Plant, J. E., and Roberts, J. J. (1971). Extension of the pre-DNA synthetic phase of the cell cycle as a consequence of DNA alkylation in Chinese hamster cells: a possible mechanism of DNA repair. *Chem. Biol. Interact.* *3*, 343–351.
- Sanchez, Y., Wong, C., Thoma, R. S., Richman, R., Wu, Z., Piwnica-Worms, H., and Elledge, S. J. (1997). Conservation of the Chk1 checkpoint pathway in mammals: linkage of DNA damage to Cdk regulation through Cdc25. *Science* *277*, 1497–1501.
- Sarkaria, J. N., Busby, E. C., Tibbetts, R. S., Roos, P., Taya, Y., Karnitz, L. M., and Abraham, R. T. (1999). Inhibition of ATM and ATR kinase activities by the radiosensitizing agent, caffeine. *Cancer Res.* *59*, 4375–4382.
- Stojic, L., Mojas, N., Cejka, P., Di Pietro, M., Ferrari, S., Marra, G., and Jiricny, J. (2004). Mismatch repair-dependent G2 checkpoint induced by low doses of SN1 type methylating agents requires the ATR kinase. *Genes Dev.* *18*, 1331–1344.
- Strausfeld, U., Labbe, J. C., Fesquet, D., Cavadore, J. C., Picard, A., Sadhu, K., Russell, P., and Doree, M. (1991). Dephosphorylation and activation of a p34cdc2/cyclin B complex in vitro by human CDC25 protein. *Nature* *351*, 242–245.
- Umar, A., Koi, M., Risinger, J. I., Glaab, W. E., Tindall, K. R., Kolodner, R. D., Boland, C. R., Barrett, J. C., and Kunkel, T. A. (1997). Correction of hyper-

- mutability, N-methyl-N'-nitro-N-nitrosoguanidine resistance, and defective DNA mismatch repair by introducing chromosome 2 into human tumor cells with mutations in MSH2 and MSH6. *Cancer Res.* 57, 3949–3955.
- Walsh, S., Margolis, S. S., and Kornbluth, S. (2003). Phosphorylation of the cyclin b1 cytoplasmic retention sequence by mitogen-activated protein kinase and Plx. *Mol. Cancer Res.* 1, 280–289.
- Wang, X., McGowan, C. H., Zhao, M., He, L., Downey, J. S., Fearn, C., Wang, Y., Huang, S., and Han, J. (2000). Involvement of the MKK6–p38gamma cascade in gamma-radiation-induced cell cycle arrest. *Mol. Cell. Biol.* 20, 4543–4552.
- Wang, Y., and Qin, J. (2003). MSH2 and ATR form a signaling module and regulate two branches of the damage response to DNA methylation. *Proc. Natl. Acad. Sci. USA*
- Wright, J. A., Keegan, K. S., Herendeen, D. R., Bentley, N. J., Carr, A. M., Hoekstra, M. F., and Concannon, P. (1998). Protein kinase mutants of human ATR increase sensitivity to UV and ionizing radiation and abrogate cell cycle checkpoint control. *Proc. Natl. Acad. Sci. USA* 95, 7445–7450.
- Xiao, Z., Chen, Z., Gunasekera, A. H., Sowin, T. J., Rosenberg, S. H., Fesik, S., and Zhang, H. (2003). Chk1 Mediates S and G2 Arrests through Cdc25A Degradation in Response to DNA-damaging Agents. *J. Biol. Chem.* 278, 21767–21773.
- Xu, B., Kim, S. T., Lim, D. S., and Kastan, M. B. (2002). Two molecularly distinct g(2)/m checkpoints are induced by ionizing irradiation. *Mol. Cell. Biol.* 22, 1049–1059.
- Yang, J., Bardes, E. S., Moore, J. D., Brennan, J., Powers, M. A., and Kornbluth, S. (1998). Control of cyclin B1 localization through regulated binding of the nuclear export factor CRM1. *Genes Dev.* 12, 2131–2143.
- Yang, J., Song, H., Walsh, S., Bardes, E. S., and Kornbluth, S. (2001). Combinatorial control of cyclin B1 nuclear trafficking through phosphorylation at multiple sites. *J. Biol. Chem.* 276, 3604–3609.
- Yu, Q., La Rose, J., Zhang, H., Takemura, H., Kohn, K. W., and Pommier, Y. (2002). UCN-01 inhibits p53 up-regulation and abrogates gamma-radiation-induced G(2)-M checkpoint independently of p53 by targeting both of the checkpoint kinases, Chk2 and Chk1. *Cancer Res.* 62, 5743–5748.
- Zampetti-Bosseler, F., and Scott, D. (1981). Cell death, chromosome damage and mitotic delay in normal human, ataxia telangiectasia and retinoblastoma fibroblasts after x-irradiation. *Int. J. Radiat. Biol. Relat. Stud Phys. Chem. Med.* 39, 547–558.
- Zhao, H., and Piwnica-Worms, H. (2001). ATR-mediated checkpoint pathways regulate phosphorylation and activation of human Chk1. *Mol. Cell. Biol.* 21, 4129–4139.
- Zhao, H., Watkins, J. L., and Piwnica-Worms, H. (2002). Disruption of the checkpoint kinase 1/cell division cycle 25A pathway abrogates ionizing radiation-induced S and G2 checkpoints. *Proc. Natl. Acad. Sci. USA* 99, 14795–14800.
- Zhou, B. B., Chaturvedi, P., Spring, K., Scott, S. P., Johanson, R. A., Mishra, R., Mattern, M. R., Winkler, J. D., and Khanna, K. K. (2000). Caffeine abolishes the mammalian G(2)/M DNA damage checkpoint by inhibiting ataxia-telangiectasia-mutated kinase activity. *J. Biol. Chem.* 275, 10342–10348.
- Zhukovskaya, N., Branch, P., Aquilina, G., and Karran, P. (1994). DNA replication arrest and tolerance to DNA methylation damage. *Carcinogenesis* 15, 2189–2194.
- Ziv, Y., Bar-Shira, A., Pecker, I., Russell, P., Jorgensen, T. J., Tsarfati, I., and Shiloh, Y. (1997). Recombinant ATM protein complements the cellular A-T phenotype. *Oncogene* 15, 159–167.